



Agnico Meliadine Mine – Meliadine Lake Hydrology Modelling

Meliadine Lake Hydrology Model Development, Calibration
and Analysis

Report
Project No 42804619-03

April 30, 2026

Prepared for Agnico Eagle



Contents

1	Introduction	1
2	Data Review	2
2.1	Surface Elevation Model.....	2
2.2	Lake Bathymetry.....	2
2.3	Lake Water Level and Flow Monitoring Data	5
2.4	Climate Data	8
3	Watershed Delineation	11
4	Model Setup	14
4.1	Terrain Data.....	14
4.2	Basin Model.....	14
4.3	Subbasins	14
4.3.1	Canopy	14
4.3.2	Snow.....	14
4.3.3	Surface Depression Storage	15
4.3.4	Catchment Runoff Flow Routing	19
4.4	Outlets.....	20
4.5	Lake Storage and Discharge.....	20
4.5.1	Elevation Area Curve.....	20
4.5.2	Discharge.....	21
4.6	Freshwater Withdraw and Effluent Discharge.....	22
4.7	Climate Data	22
5	Model Calibration	24
5.1	Calibration Period	24
5.2	Model Calibration Process.....	24
5.3	Model Calibration Result	25
5.4	Model Validation Result.....	27
6	Projected Inflow and Lake Levels for the Future Mine Operations Period (2026-2036) ..	29
6.1	Future Model Scenarios	32
6.2	Model Results	32
7	Mine Closure 2037-2043	35
7.1	Model Scenarios.....	35
7.2	Model Results	35
8	Conclusions	37
9	References	38

Figures

Figure 2-1	Digital Surface Model and Tiles for Meliadine Lake.....	3
Figure 2-2	Bathymetry Map for Meliadine Lake and Peninsula Lakes.....	4
Figure 2-3	Measured Lake Level and Discharge at Main Outlet and West Outlet (1997 to 2000)	6
Figure 2-4	Measured Lake Level and Discharge at Main Outlet and West Outlet (2024 to 2025)	6

Figure 2-5 Converted Water Level Data from 1997 to 2000.....	7
Figure 2-6 Climate data at Camp Station and Rankin Station.....	8
Figure 2-7 Annual Precipitation at Rankin Station from 1996 to 2024	9
Figure 2-8 Daily Precipitation Depth and Cumulative Precipitation at Camp Station and Rankin Station from 2021 to 2025	9
Figure 2-9 Lake Evaporation at Camp Station.....	10
Figure 3-1 Pour Points and Catchments.....	13
Figure 4-1 Map of the Meliadine Lake HEC-HMS Model Including the Subbasins Boundaries and Connection to Meliadine Lake.....	16
Figure 4-2 Estimated Storage Depth in Topographic Depression (Sinks).....	18
Figure 4-3 Elevation Area Curve of Meliadine Lake	21
Figure 4-4 Elevation Discharge Curves for Main Outlet and West Outlet	22
Figure 4-5 Time-Series Plot of Daily Effluent Discharge to Meliadine Lake.....	23
Figure 4-6 Time-Series Plot of Daily Freshwater Withdraw from Meliadine Lake.....	23
Figure 5-1 Modeled and Measured Lake Level (Aug 25, 2024 to Sep 24, 2025)	27
Figure 5-2 Modeled and Measured Lake Level (Sep 1, 1996 to Oct 1, 2000)	28
Figure 6-1 Precipitation from 2026 to 2050.....	29
Figure 6-2 Accumulative Precipitation from 2020 to 2025 for Climate Change Scenarios and Rankin Station	30
Figure 6-3 Average Monthly PET.....	31
Figure 6-4 Average Annual PET	31
Figure 6-5 Meliadine Lake Level and Inflow for Existing and Maximum Withdrawal Scenarios (2026-2036, RCP 4.5).....	33
Figure 6-6 Meliadine Lake Level and Inflow for Existing and Maximum Withdrawal Scenarios (2026-2036, RCP 6.0).....	33
Figure 6-7 Meliadine Lake Level and Inflow for Existing and Maximum Withdrawal Scenarios (2026-2036, RCP 8.5).....	34
Figure 6-8 Meliadine Lake Level and Inflow for Maximum Withdrawal Scenario (2026-2036, RCP 4.5, RCP 6.0 and RCP 8.5).....	34
Figure 7-1 Lake Level and Inflow for June-Sept Withdrawal Scenario for RCP 4.5, RCP 6.0 and RCP 8.5	36

Tables

Table 3-1 Summary of Meliadine Lake Watershed Subbasin Areas.....	12
Table 4-1 Snow Parameters	14
Table 4-2 Wet and Dry Melt Rate.....	15
Table 4-3 Subbasin Storage Estimates	17
Table 4-4 Summary of Subbasin Time of Concentration and Storage Coefficient Estimates.....	19
Table 5-1 Calibrated Wet and Dry Melt Rate.....	24
Table 5-2 Calibrated Subbasin Storage and Storage Coefficient.....	25
Table 6-1 Statistics of Lake Water Level and Outflow for the Period from 2026-2036	33
Table 7-1 Statistics of Lake Water Level and Outflow for Mine Closure Analysis.....	35

1 Introduction

Located near the western shore of Hudson Bay in the Kivalliq District of Nunavut, the Meliadine Mine is owned by Agnico Eagle Mines Limited (Agnico Eagle) and began commercial production in May 2019. Under the current mine plan, operations will continue until 2036. To support ongoing operations and camp requirements, annual freshwater demand is expected to increase by approximately 10,000 m³/year. The mine is currently authorized to withdraw up to 1,100,296 m³ of freshwater per year. To accommodate the increased water demand, Agnico Eagle will be submitting a water license amendment for the additional withdrawal, resulting in a proposed total annual freshwater withdrawal of approximately 1,110,296 m³/year. Once the mine closes at the end of 2036, Agnico Eagle plans to increase the annual volume of freshwater withdrawal from Meliadine Lake to 8,700,000 m³ from 2037-2043.

Agnico Eagle has contracted DHI Water & Environment, Inc. (DHI) to provide professional services in support of the Meliadine Water License Amendment. The scope of work focuses on hydrological modelling to characterize runoff into Meliadine Lake for historical climate conditions and to the model to predict runoff and lake levels for future climate conditions during the mine operations and after closure. The objectives of the project are as follows:

- Develop a hydrology model of the entire Meliadine Lake watershed
- Calibrate and validate this model against historical data
- Quantify the runoff entering Meliadine Lake for a future 17-year period (2026-2043) using future climate data.
- Assess the potential effects of freshwater withdrawals on Meliadine Lake water levels during the mine operating period from 2026-2036.
- Assess the potential effects of freshwater withdrawals on the Meliadine Lake water levels during the mine closure period from 2037-2043.

This report provides a description of the work completed by DHI to meet the objectives of this project.

2 Data Review

The following section describes the data and processing that was used for the development and calibration of the Meliadine Lake watershed hydrology model.

2.1 Surface Elevation Model

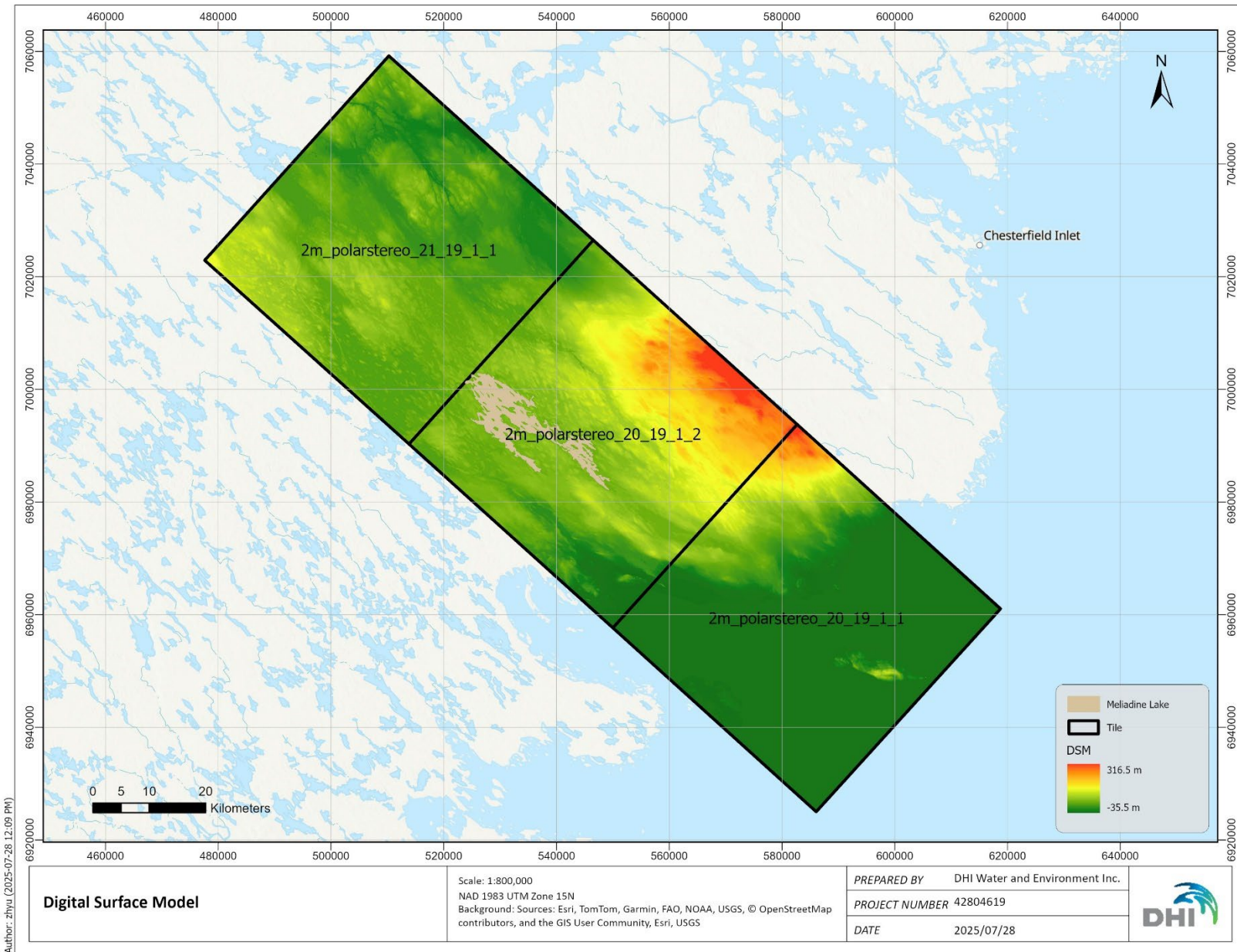
From [High Resolution Digital Elevation Model \(HRDEM\) Open Maps portal](#), the 2m-resolution Digital Surface Model (DSM) dataset was downloaded for the following three tiles.

- 2m_polarstereo_21_19_1_1
- 2m_polarstereo_20_19_1_2
- 2m_polarstereo_20_19_1_1

The DSM data and tile boundary is shown in Figure 2-1. The data files are in GeoTIFF format. They were merged to a single file and resampled to 30m resolution for watershed delineation.

2.2 Lake Bathymetry

Bathymetry Triangular Irregular Network (TIN) data for Meliadine Lake is shown in Figure 2-2. The water depth contour lines were also provided for some of the Peninsula Lakes and included in Figure 2-2.



Author: zhyu (2025-07-28 12:09 PM)

Figure 2-1 Digital Surface Model and Tiles for Meliadine Lake

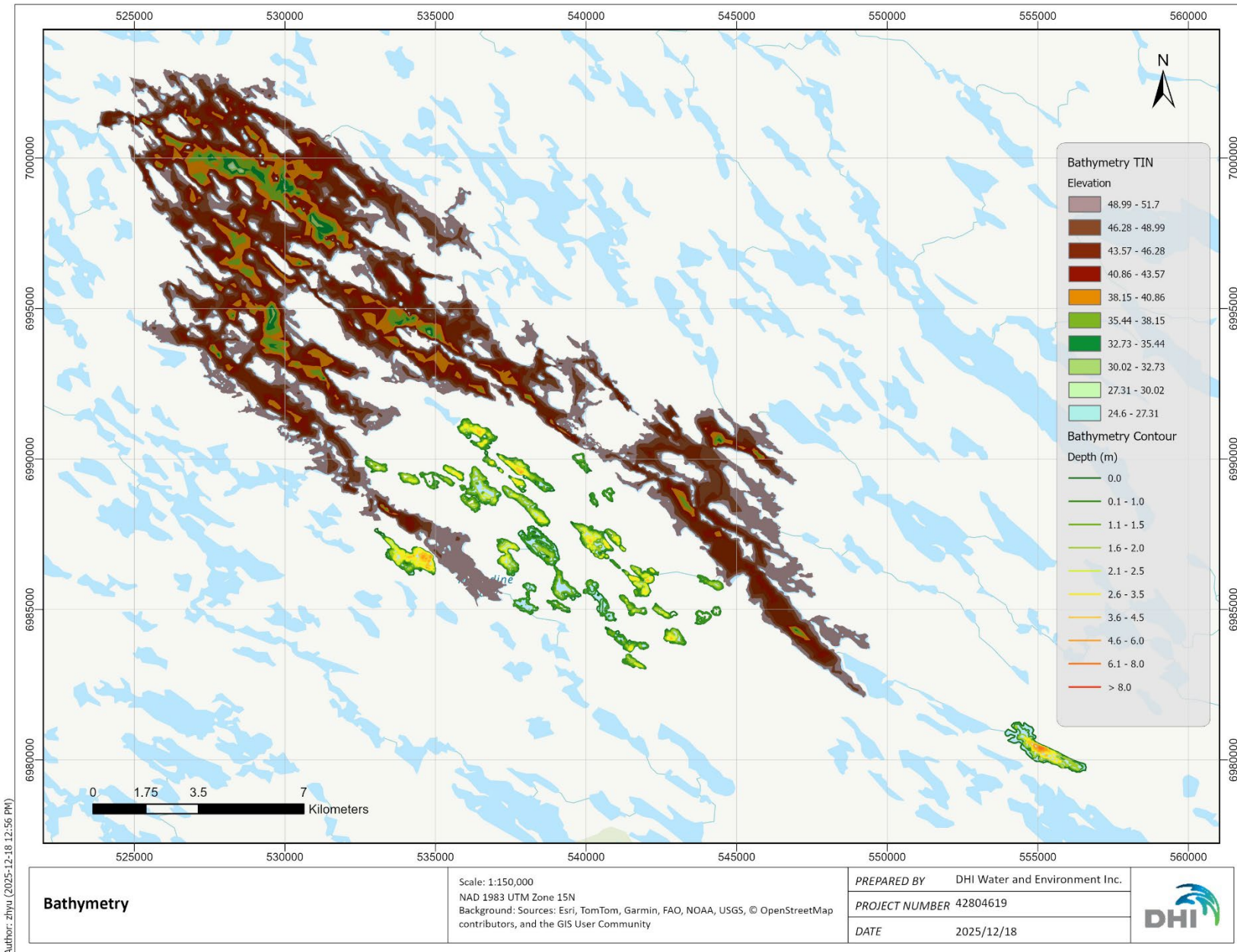


Figure 2-2 Bathymetry Map for Meliadine Lake and Peninsula Lakes

2.3 Lake Water Level and Flow Monitoring Data

The discharge at main outlet and west outlet and the water level in Meliadine Lake were provided for the following three periods:

- From 1997 to 2000, and
- From 2024 to 2025.

The data are plotted in Figure 2-3 to Figure 2-5. In 2008, the discharge data are only available for three days and water level data are only available for August.

The water level data in these three periods used a different reference system for the stage. Agnico Eagle staff confirmed that the water level data from 2024 to 2025 are geodetic elevations. The reference elevations for 1997-2000 dataset is unknown. For the period 1997 to 2000, the reference elevation was assumed to be 48.27m so the lowest water level in 2000 is same as the lowest water level in 2025. With this reference elevation, the water level data from 1997 to 2000 were converted to elevation as shown in Figure 2-6.

The discharge at the main outlet and west outlet were derived from rating curves. The rating curves for the 2024-2025 monitoring program are given below, where *Level* is the lake level in m. The rating curves for 1997-2000 and 2008 are unknown.

- Main Outlet: $2^{-144}e^{6.4276Level}$
- West Outlet: $4^{-215}e^{9.5692Level}$

The rating curves were developed using measurements collected during the open-water season (June to September) and may not be applicable under winter conditions where thick ice cover is predominant throughout the lake and the outlet watercourses. The Aquatic Baseline Synthesis Report (Golder Associates, 2012) notes that ice thickness in some small lakes can reach 1.5–1.7 m. Ice of this thickness traps water within the ice matrix and potentially obstructs outflow pathways. As such, the outflow rating curve developed using measurements collected during open water season may not be representative of outflow conditions during winter conditions where thick ice cover prevails.

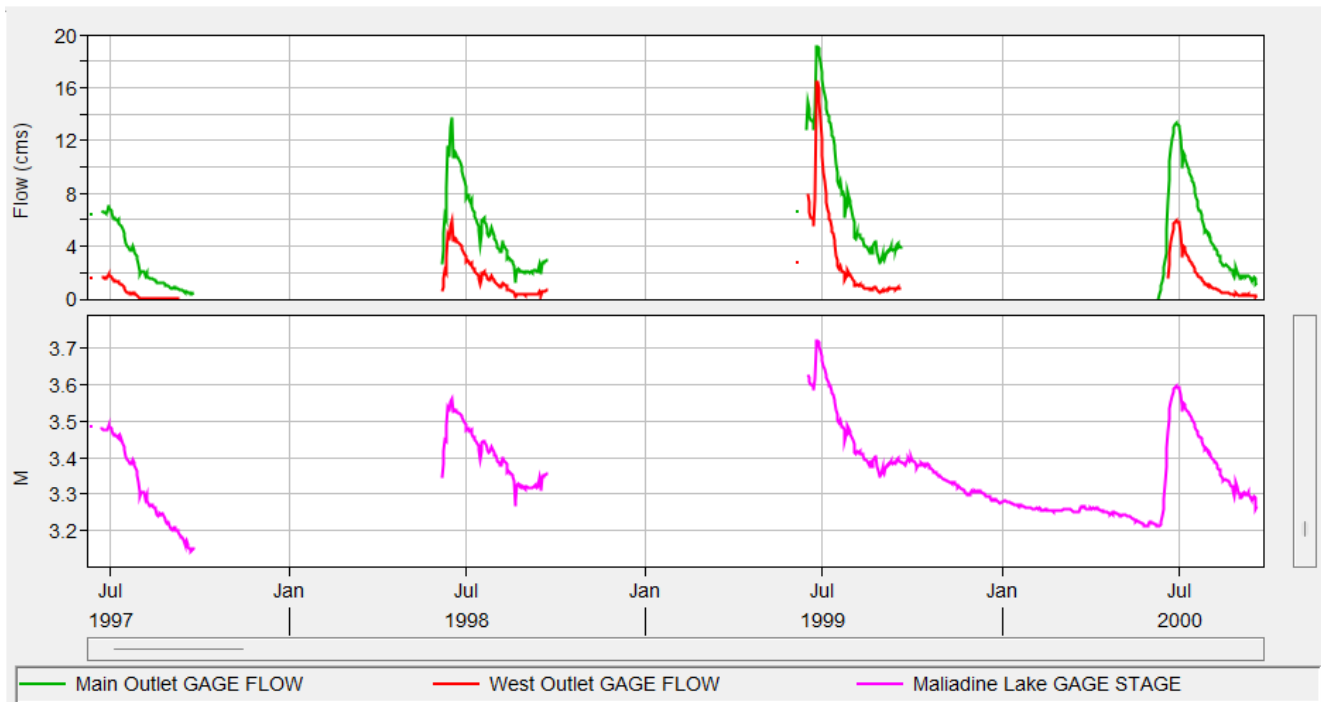


Figure 2-3 Measured Lake Level and Discharge at Main Outlet and West Outlet (1997 to 2000)

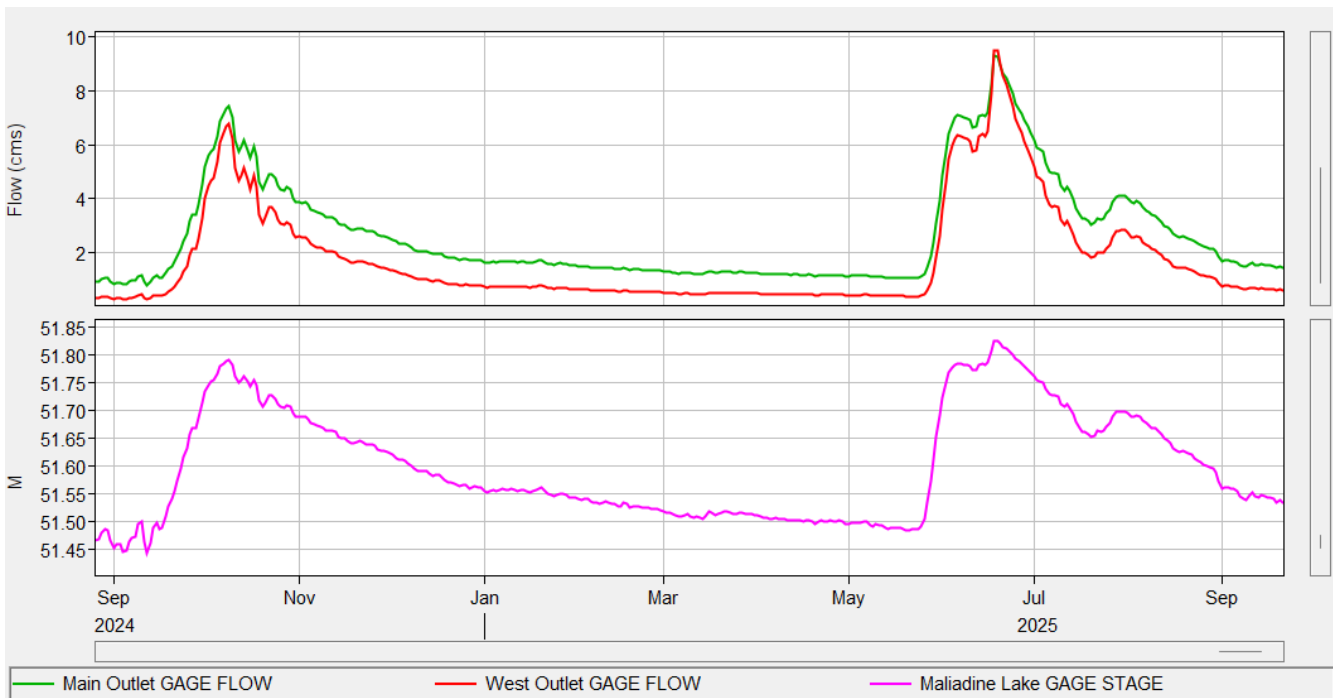


Figure 2-4 Measured Lake Level and Discharge at Main Outlet and West Outlet (2024 to 2025)

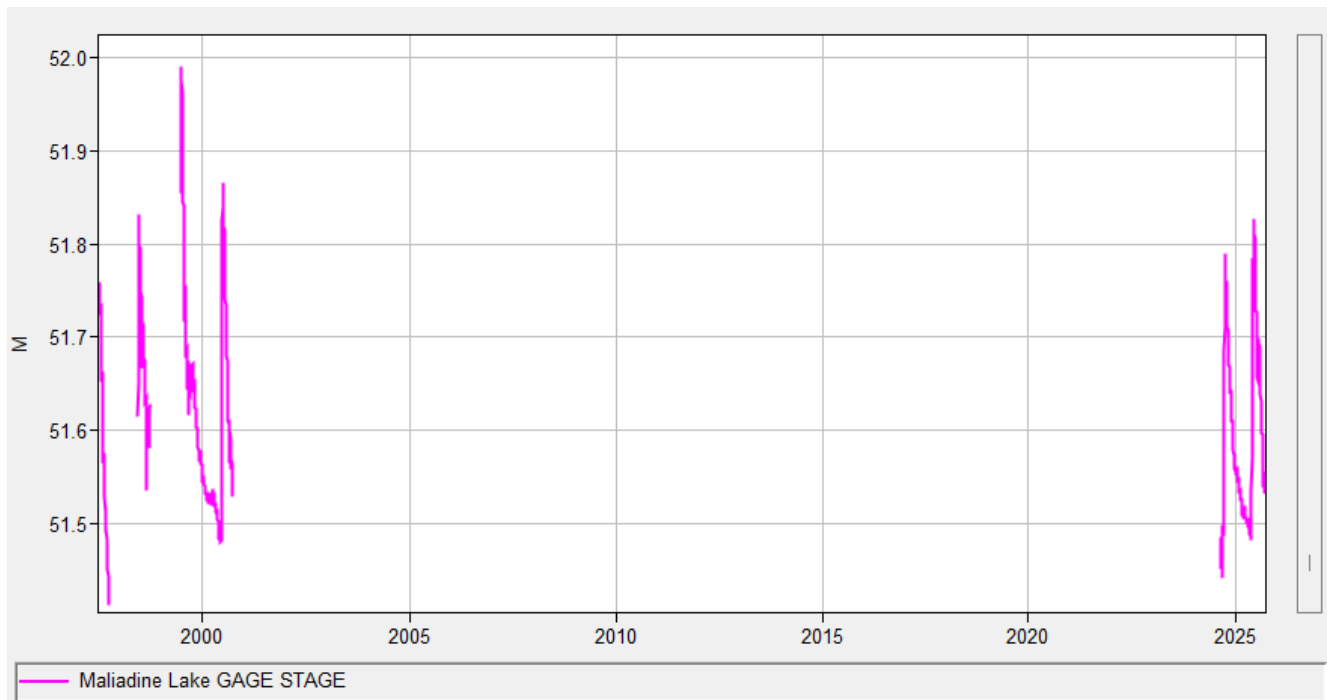


Figure 2-5 Converted Water Level Data from 1997 to 2000

2.4 Climate Data

A rain gauge was installed at Meliadine Camp (Camp Station) and collected rainfall data during the open season in 2000, 2008 and 2009 and continuously from November 1st, 2020 to 2025. Continuous climate data has been available at Rankin Inlet Airport (Rankin Station) since 1981. The Rankin Station is located about 30 km southeast of Meliadine Gold Mine, closer to the ocean. The daily precipitation and temperature data from Rankin was downloaded and plotted together with the precipitation data at Camp Station in Figure 2-7. The temperature data shows that the temperature is generally above zero Celsius from June to September.

The annual precipitation at Rankin Station from 1996 to 2024 is plotted in Figure 2-8 with an average annual precipitation of 302mm.

The cumulative precipitation measurements recorded from 2021 to 2025 at the Rankin Station and the Camp Station are compared in Figure 2-10. The cumulative curves for both stations follow a similar pattern and remain closely aligned throughout most of the period where overlapping data is available. One notable exception occurred on June 8, 2023 where the Camp Station recorded a precipitation depth of 50.69 mm while the Rankin station recorded missing data during that period (see circled event in Figure 2-10). This difference caused the cumulative precipitation curves to diverge on June 8, 2023 but, otherwise, the two curves are almost identical before and after this event. It should be noted that this particular event does not affect the hydrological modelling because it was not used for the model calibration or validation.

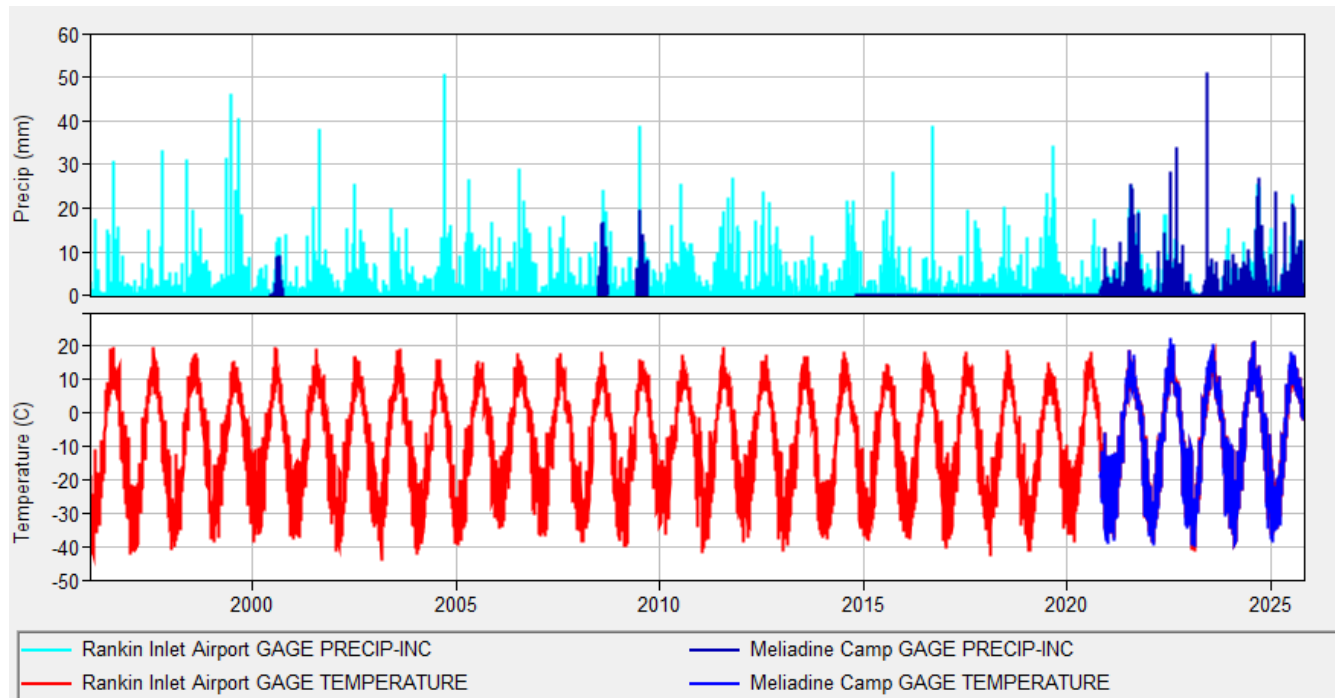


Figure 2-6 Climate data at Camp Station and Rankin Station

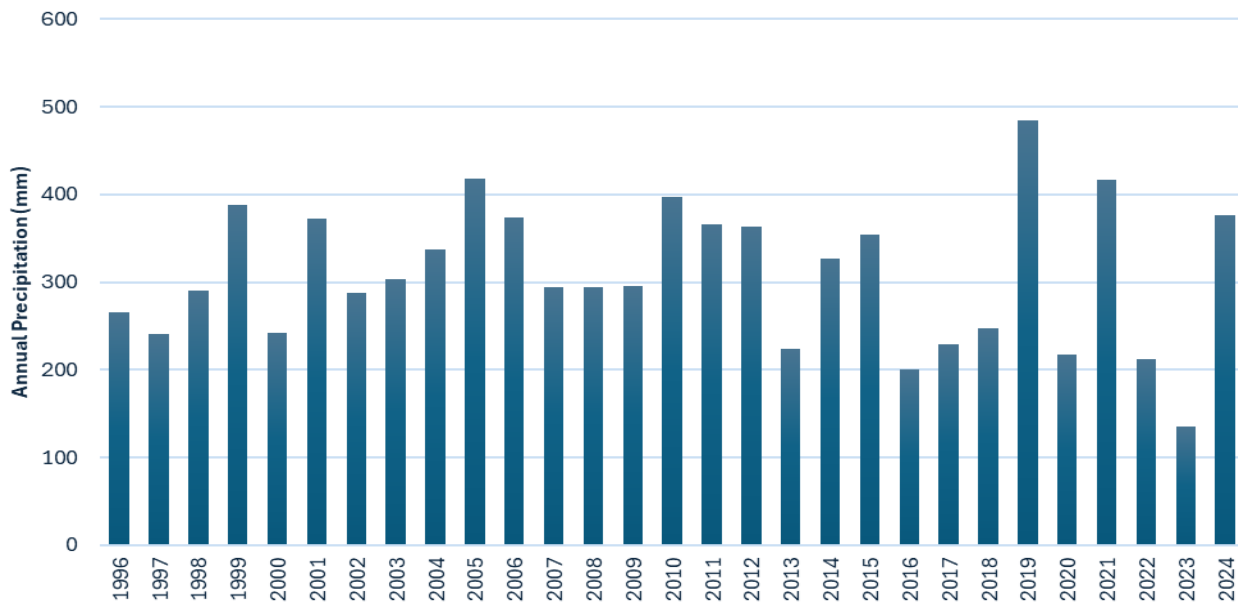


Figure 2-7 Annual Precipitation at Rankin Station from 1996 to 2024

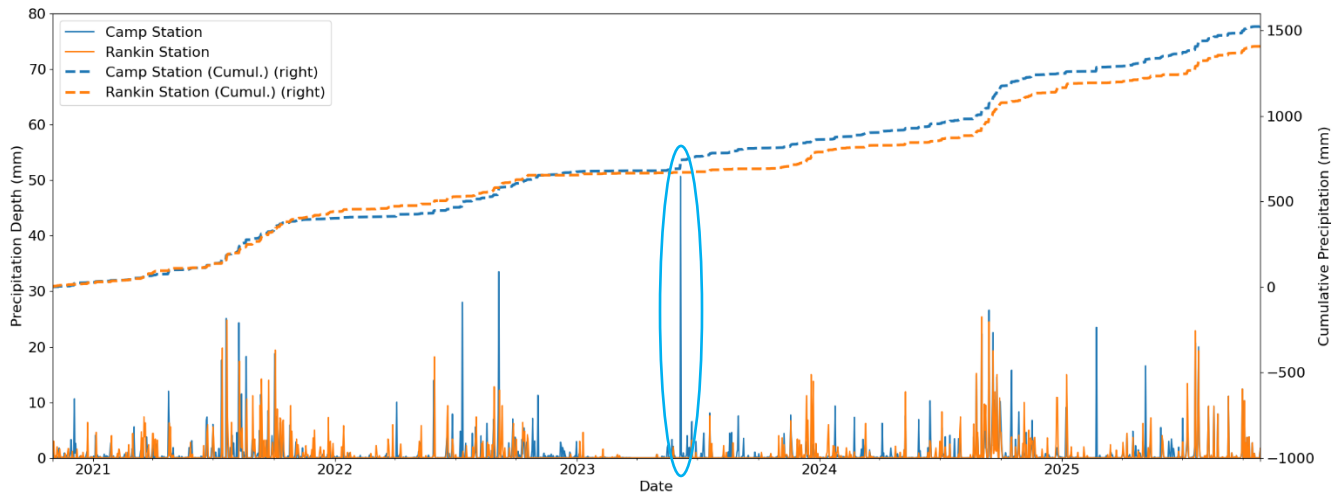


Figure 2-8 Daily Precipitation Depth and Cumulative Precipitation at Camp Station and Rankin Station from 2021 to 2025

Pan evaporation and lake evaporation data were collected at Camp Station from 1997 to 2000. The lake evaporation data is shown in Figure 2-11. Negative values were found in the Lake evaporation data and have been removed for plotting purposes. From the measured data, the average monthly lake evaporation was provided in the Aquatic Baseline Synthesis Report, 1994 to 2009 (Golder Associates, 2012) as listed below.

- June: 60.4 mm
- July: 124.4 mm
- August: 95.6 mm
- September: 42.7 mm
- Annual: 323 mm

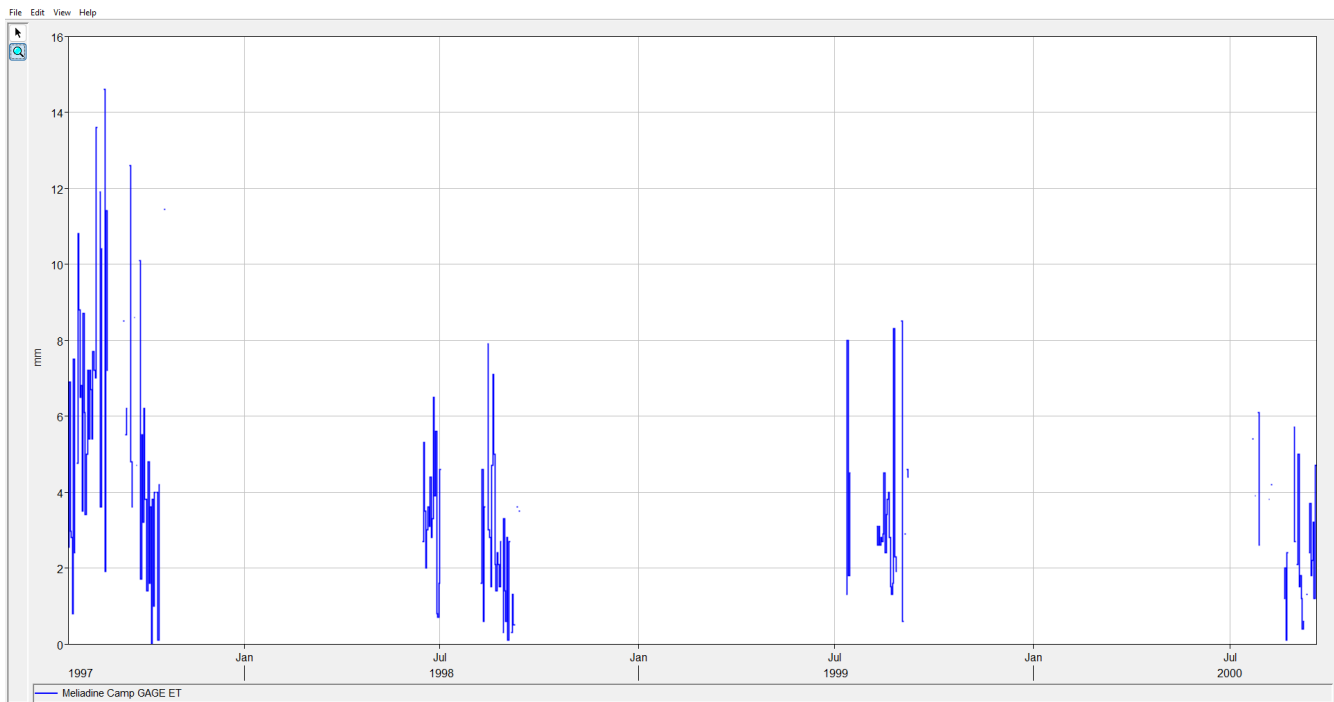


Figure 2-9 Lake Evaporation at Camp Station

3 Watershed Delineation

The 30-m resolution DSM GeoTIFF file was used to delineate subbasins within the Meliadine Lake watershed. A minimum threshold area of 1 km² was applied to define the stream network and subbasin areas. Following the identified streams, 33 pour points were established at Meliadine Lake outlets and major inlets to the Lake. These pour points were then used to delineate 33 corresponding subbasins. The resulting stream network and subbasin boundaries are presented in Figure 3-1.

The subbasins were named after the grid code of pour points starting from 0. For example, subbasin 'Sub6' corresponds to pour point with grid code of pour point 6. The subbasin for Meliadine Lake was named as SubLake and the catchments for the Peninsula Lakes were named after the name of the zone (e.g. A, B, C, etc.). The area of the subbasins is listed in Table 3-1 from the largest to the smallest. The largest subbasin is 187.91 km² and the smallest is 1.12 km². The subbasin for Meliadine Lake (SubLake) includes both Meliadine Lake and adjacent contribute areas that are too small to be separated as catchments. The total drainage area of the Meliadine Lake watershed is 588.82 km².

Table 3-1 Summary of Meliadine Lake Watershed Subbasin Areas

Index	Name	Area (km ²)
1	Sub6	187.91
2	SubLake	178.59
3	Sub8	52.18
4	B	19.65
5	Sub12	17.71
6	Sub9	14.61
7	Sub21	10.26
8	A	9.74
9	Sub17	9.20
10	Sub7	8.79
11	D	7.70
12	C	7.58
13	Sub23	7.30
14	O	6.40
15	Sub14	5.64
16	Sub24	5.16
17	E	3.78
18	Sub15	3.33
19	Sub18	3.23
20	Sub30	3.16
21	Sub10	3.13
22	Sub22	2.96
23	Sub19	2.76
24	Sub20	2.62
25	Sub11	2.49
26	H	2.27
27	F	2.24
28	Sub28	2.12
29	J	1.47
30	Sub16	1.26
31	Sub26	1.24
32	Sub29	1.20
33	G	1.12
Total		588.82

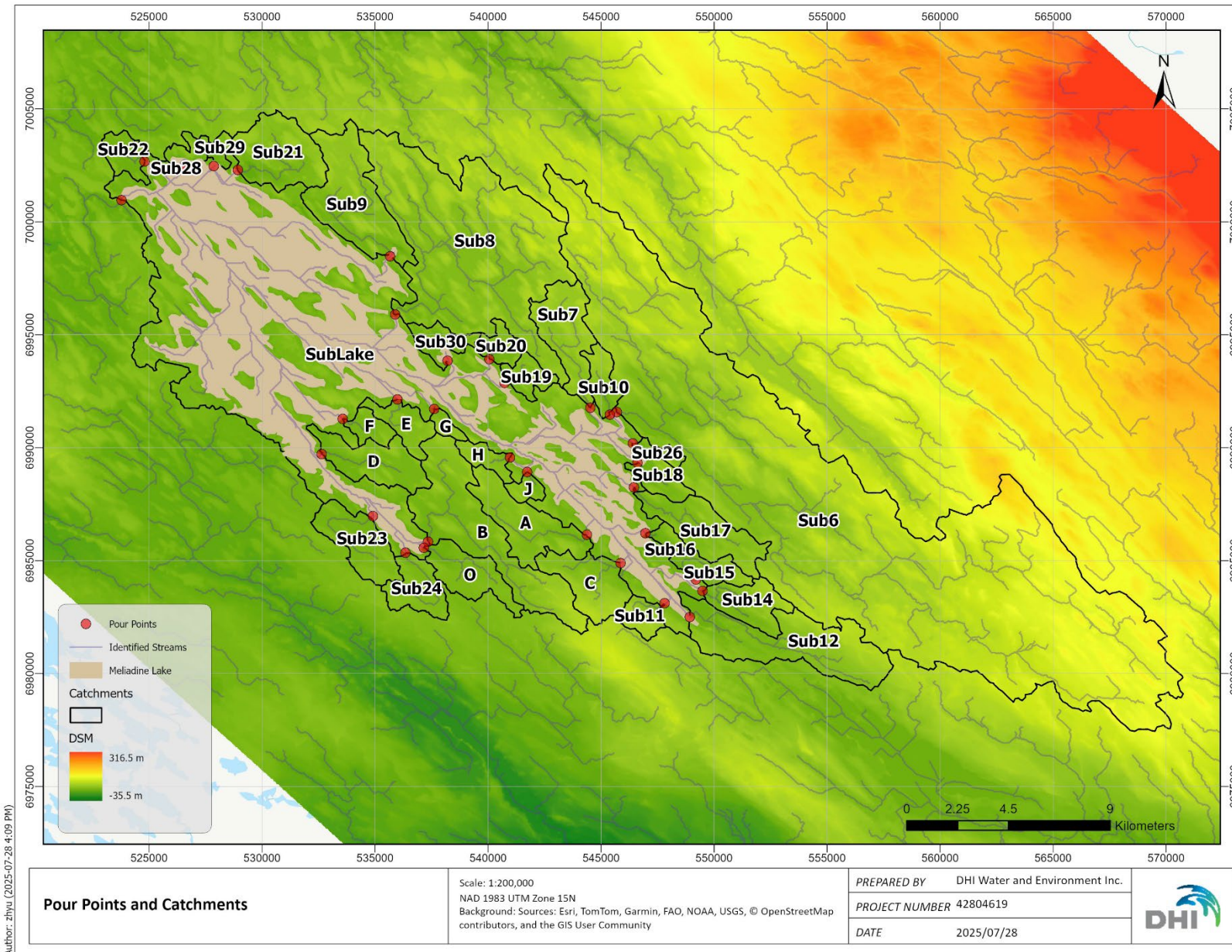


Figure 3-1 Pour Points and Catchments

4 Model Setup

The Meliadine Lake watershed hydrology model was setup using the HEC-HMS model.

4.1 Terrain Data

The 30-m resolution DSM GeoTIFF file is added to HEC-HMS model as the terrain data.

4.2 Basin Model

A HEC-HMS basin model was created for this project with name “Meliadine Lake” as shown in Figure 4-1. It was connected to the terrain data, and the coordinate system was set as NAD83 UTM 15N. Three HEC-HMS GIS commands were used to process the terrain data. A minimum threshold of 1km² was used for identifying streams and delineating subbasins. The terrain data is not reconditioned because the stream data is not available. The Meliadine Lake boundary (purple) were also added to the map as background layer.

4.3 Subbasins

The delineated subbasins were imported to HEC-HMS using “Import Georeferenced Elements” command. Subbasins were created automatically for each catchment and the ID and area are automatically populated. The subbasin boundary and icons are shown in Figure 4-1.

4.3.1 Canopy

As the study area is primarily permafrost and above the tree line, The Canopy Method was set to none. No interception and transpiration was modeled.

4.3.2 Snow

Temperature Index method was used to model the snow process for all subbasins. The common parameters are listed in Table 4-1. An annual pattern was used for both wet melt and dry melt. The monthly melt rates are provided in Table 4-2. Same values were used for both wet melt and dry melt.

Table 4-1 Snow Parameters

Parameter Name	Values
Snow/rain discriminating temperature (PX temperature)	0°C
Snow melt temperature (Base Temperature)	0°C
Rain rate lime	5 mm/day
Antecedent temperature index-meltrate coefficient	0.98
Cold Limit	125 mm/day
Antecedent temperature index-coldrate coefficient	0.5
Liquid water capacity	5%
Groundmelt Rate	0 mm/day

Table 4-2 Wet and Dry Melt Rate

Month	Melt Rate (mm/°C-day)	Month	Melt Rate (mm/°C-day)
January	1	July	4.5
February	1.5	August	5
March	2	September	4
April	3	October	3
May	4	November	2
June	4.5	December	1

As the elevation difference in the drainage area is below 100m, a single elevation band was used in each subbasin with initial values set to zero.

4.3.3 Surface Depression Storage

The Simple Surface method was used to model the surface depression storage in each subbasin. To estimate the available storage of each subbasin (excluding Meliadine Lake, since the storage is modelled as a Reservoir), the HEC-HMS Preprocess Sinks command was used to calculate the maximum depth of available storage in each sink (see Figure 4-2). The total volume of the sinks (i.e. surface depressions) in each subbasin was then calculated and divided by subbasin area to get an estimate of the available surface depression storage depth (in mm) in each subbasin (see summary in Table 4-3).

Figure 4-2 shows that the sink locations captured most of the water bodies by comparing to the background map. However, it is clear that some large water bodies in subbasins Sub6 and Sub8 are not captured. In addition, some sink depth values (red colors) in subbasins Sub12, Sub14, and Sub6 are unusually large compared to the majority of sinks. To avoid unreasonably large storage values, the storage value of subbasin A (38mm) was applied for subbasins Sub12 and Sub14.

The subbasin storage estimates provided in Table 4-3 were then adjusted during the model calibration process.

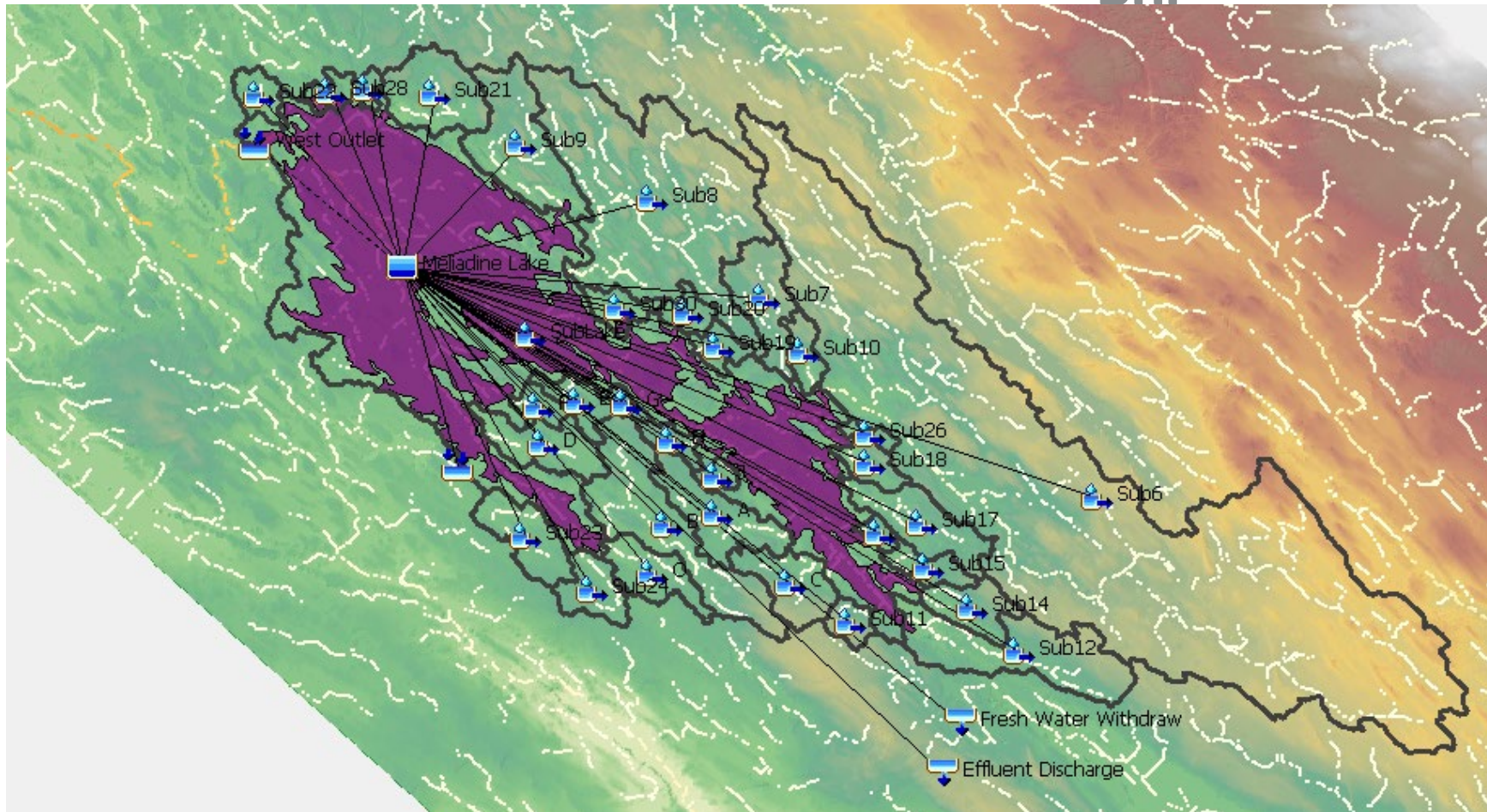


Figure 4-1 Map of the Meliadine Lake HEC-HMS Model Including the Subbasins Boundaries and Connection to Meliadine Lake

Table 4-3 Subbasin Storage Estimates

Index	Subbasin	Max Storage (mm)
1	Sub6	91
2	Sub8	28
3	B	41
4	Sub12	38
5	Sub9	93
6	Sub21	51
7	A	38
8	Sub17	91
9	Sub7	52
10	D	38
11	C	10
12	Sub23	35
13	O	31
14	Sub14	38
15	Sub24	20
16	E	49
17	Sub15	69
18	Sub18	35
19	Sub30	66
20	Sub10	13
21	Sub22	105
22	Sub19	19
23	Sub20	5
24	Sub11	43
25	H	20
26	F	16
27	Sub28	95
28	J	7
29	Sub16	23
30	Sub26	5
31	Sub29	43
32	G	9

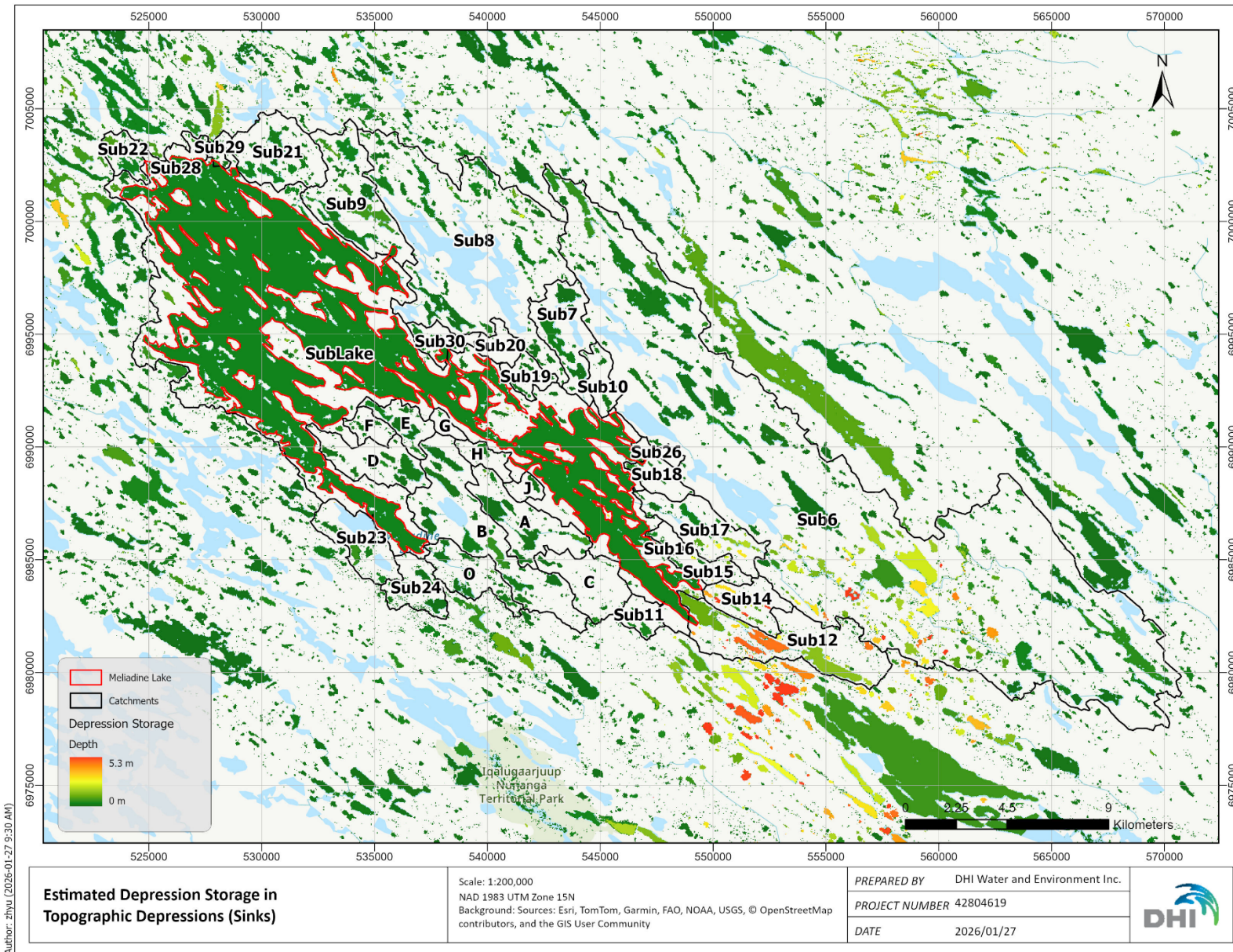


Figure 4-2 Estimated Storage Depth in Topographic Depression (Sinks)

4.3.4 Catchment Runoff Flow Routing

Transform process calculates the surface runoff from excess rainfall and/or snow melt. The Clark Unit Hydrograph method was selected to model this process. The two key parameters are time of concentration and storage coefficient.

As the initial estimation, the time of concentration is calculated using the Williams formula given below.

$$t_c = 0.057LA^{-0.1}S^{-0.2}$$

where

t_c = time of concentration (min)

L = longest flow path (m)

A = subbasin area (ha)

S = average slope

With the terrain data, L , A and S was calculated with command in Parameters -> Characteristics -> Subbasin. These values were then used to calculate the time of concentration as listed in Table 4-4.

The initial estimates of storage coefficient were calculated as $\frac{13}{7} * t_c$ following the example in HEC-HMS tutorial (HEC-HMS Team, 2025). The calculated values are listed in Table 4-4.

Table 4-4 Summary of Subbasin Time of Concentration and Storage Coefficient Estimates

Index	Subbasin	Time of Concentration (hr)	Storage Coefficient (hr)
1	Sub6	11.2	20.8
2	Sub8	6.3	11.6
3	B	4.4	8.2
4	Sub12	4.7	8.8
5	Sub9	3.9	7.2
6	Sub21	2.6	4.9
7	A	3.4	6.3
8	Sub17	3.6	6.8
9	Sub7	3.4	6.2
10	D	2.5	4.6
11	C	2.0	3.7
12	Sub23	3.1	5.7
13	O	3.2	6.0
14	Sub14	2.2	4.2
15	Sub24	3.4	6.2
16	E	1.8	3.4
17	Sub15	2.6	4.8
18	Sub18	1.6	2.9
19	Sub30	1.2	2.2
20	Sub10	1.8	3.3

21	Sub22	1.4	2.5
22	Sub19	1.6	2.9
23	Sub20	1.1	2.0
24	Sub11	1.8	3.3
25	H	1.6	2.9
26	F	1.6	2.9
27	Sub28	1.3	2.4
28	J	1.7	3.2
29	Sub16	1.1	2.0
30	Sub26	1.3	2.4
31	Sub29	1.1	2.0
32	G	1.1	2.0

4.4 Outlets

There are two known outlets for Meliadine Lake; Main Outlet, and West Outlet. These outlets are modelled as sinks in HEC-HMS. They were placed in the model according to their spatial location as shown in Figure 4-1.

4.5 Lake Storage and Discharge

The storage and discharge of Meliadine Lake is modelled using a Reservoir component. Since the lake has two outlets (Main Outlet and West Outlet), the Outflow Structure was used to represent the outlets because it allows the model to represent an Auxiliary Discharge in addition to the Primary Discharge. The Primary Discharge (solid connection line in Figure 4-1) was set to Main Outlet and the Auxiliary Discharge (dash connection line in Figure 4-1) is set to West Outlet.

4.5.1 Elevation Area Curve

The storage method was set to Elevation-Area and the elevation area curve is shown in Figure 4-3. It was derived using the Surface Volume tool in ArcGIS Pro for each 0.1m incremental water depth based on the Triangulated Irregular Network (TIN) dataset of Meliadine Lake. As the maximum elevation in the TIN dataset (51.7m) is lower than the peak measured water level (51.8m), additional elevation-area values were calculated using the 2-m resolution DSM data. Compared to the TIN dataset, the DSM data produced larger surface area for the same elevation, which leads to a jump near 51.7m.

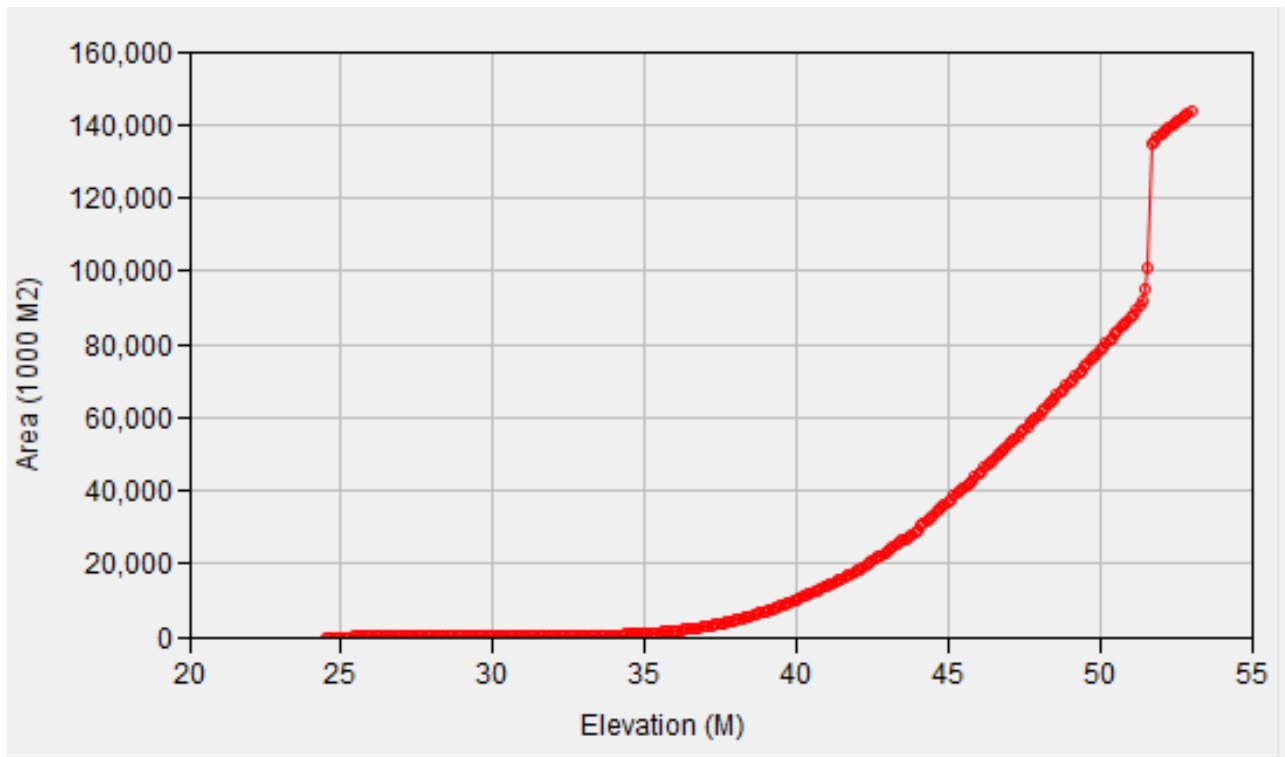


Figure 4-3 Elevation Area Curve of Meliadine Lake

4.5.2 Discharge

The discharge from Main Outlet and West Outlet was modelled using Elevation-Discharge curves. Two spillways were added to the Reservoir; one for the Main Outlet and one for the West Outlet. The discharge method of the spillways was set to Specified Spillway. The Elevation-Discharge curve values were calculated using the regression equation described in Section 2.3 and shown in Figure 4-4.

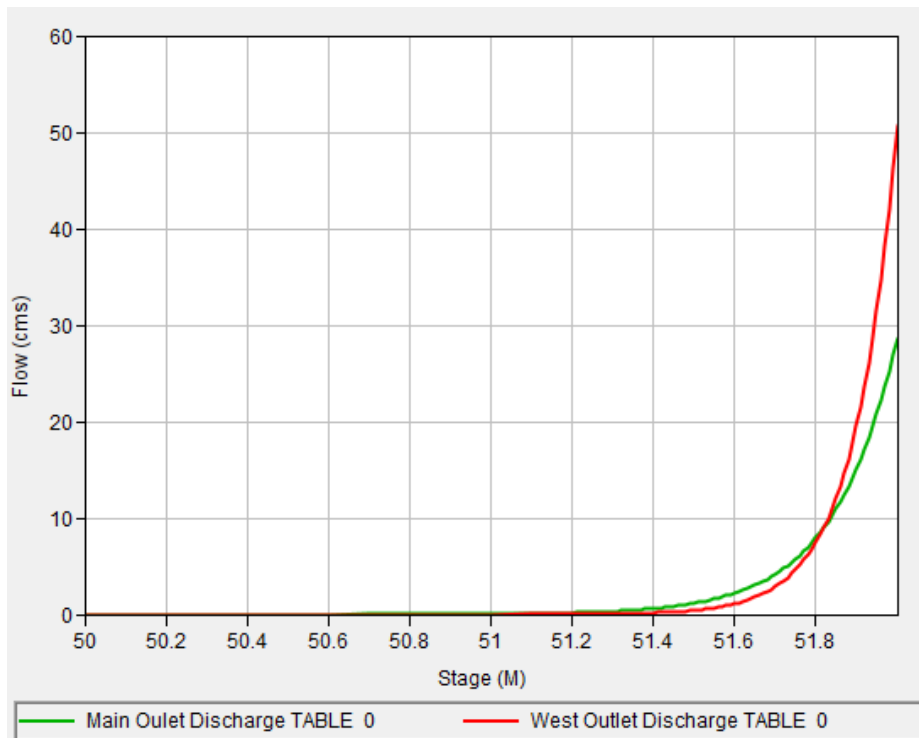


Figure 4-4 Elevation Discharge Curves for Main Outlet and West Outlet

4.6 Freshwater Withdraw and Effluent Discharge

As shown in Figure 4-5 and Figure 4-6, the freshwater withdrawal and effluent discharge were derived from the 2024 monthly water volume records (Agnico Eagle, 2024). A total of 519,502 m³ was withdrawn during the year while a total of 816,476 m³ of effluent was discharged into the lake. For the purposes of using this for the model calibration, it was assumed the water volumes were evenly distributed through the months, and the same flow pattern was repeated for each year that was evaluated for the model calibration and validation. The freshwater withdrawal was modeled as an additional release from the lake with a specific outflow rate, and the effluent discharge was modelled as a source.

4.7 Climate Data

The Meliadine Lake watershed hydrology model was setup to run two different climate data scenarios; one that uses precipitation and temperature data from the Camp Station; and the other uses precipitation and temperature data from the Rankin Station. Both of the calibration period climate scenarios used the same evapotranspiration data discussed in Section 2.4. The purpose of using these two scenarios was to evaluate the model calibration using different potential climate data sets.

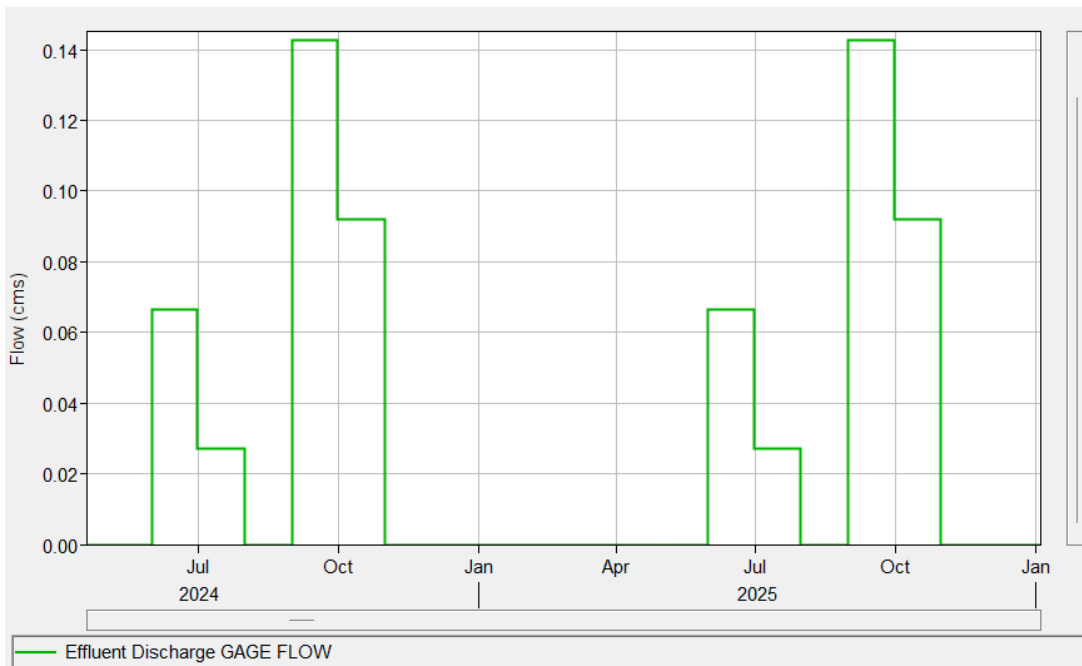


Figure 4-5 Time-Series Plot of Daily Effluent Discharge to Meliadine Lake

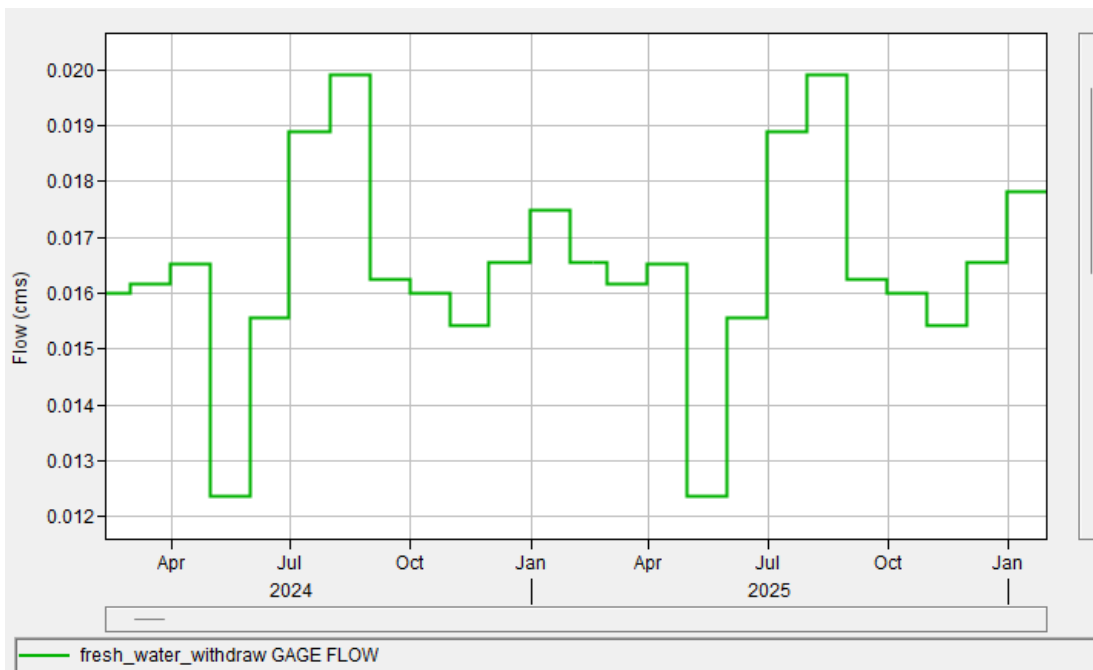


Figure 4-6 Time-Series Plot of Daily Freshwater Withdraw from Meliadine Lake

5 Model Calibration

5.1 Calibration Period

Based on data availability, two periods were selected for model calibration and validation.

- **Calibration: Aug 25, 2024 to Sep 24, 2025:** This is the latest dataset with continuous lake level measurement given in elevations. The precipitation data at Camp Station and Ranking Station covers the entire period. The outlet flow rating curves used in the model are also based on the measurements done during this period.
- **Validation: Sep 1, 1996 to Oct 1, 2000:** This period was used for validation because it was the only other period with suitable data available. However, the lake level data measured during this period didn't have a clear reference elevation, and the rainfall data at Camp Station is not continuous for the period. Continuous climate data for this period was available from the Rankin Station.

5.2 Model Calibration Process

The model was mainly calibrated to the measured lake level during the calibration period as this was the only continuous measurement available.

The model parameters that were adjusted during the calibration process included snowmelt parameters, storage coefficient, and storage depth. Since there was only a single location of calibration, and since there isn't much orographic relief throughout the watershed, the snowmelt parameters are applied uniformly across all subbasins. Similarly, the adjustments to the storage coefficient and storage depth were applied proportionally across all subbasins (the values were all adjusted by the same factor).

The adjustments were applied until a suitable match was achieved between the measured and modelled water level of Meliadine Lake. The calibrated snowmelt parameters, as well as the storage coefficient values and storage depth values for each subbasin are provided in Table 5-1 and Table 5-2. The calibration results are described in the following section.

Table 5-1 Calibrated Wet and Dry Melt Rate

Month	Melt Rate (mm/°C-day)	Month	Melt Rate (mm/°C-day)
January	1	July	4.5
February	1.5	August	5
March	2	September	4
April	3	October	3
May	3	November	2
June	5	December	1

Table 5-2 Calibrated Subbasin Storage and Storage Coefficient

Index	Subbasin	Max Storage (mm)	Storage Coefficient (Hour)
1	Sub6	70	750
2	Sub8	22	418
3	B	32	295
4	Sub12	32	317
5	Sub9	72	259
6	Sub21	39	176
7	A	29	227
8	Sub17	70	245
9	Sub7	40	223
10	D	29	166
11	C	8	133
12	Sub23	27	205
13	O	24	216
14	Sub14	32	151
15	Sub24	15	223
16	E	38	122
17	Sub15	53	173
18	Sub18	27	104
19	Sub30	51	79
20	Sub10	10	119
21	Sub22	81	90
22	Sub19	15	104
23	Sub20	5	72
24	Sub11	33	119
25	H	15	104
26	F	12	104
27	Sub28	73	86
28	J	5	115
29	Sub16	18	74
30	Sub26	5	87
31	Sub29	33	74
32	G	7	74

5.3 Model Calibration Result

The modelled and measured lake levels for the calibration period are shown in Figure 5-1. Two model simulations are presented: one shows the hydrological modelling results using precipitation data from the

Camp Station (blue) and the other using precipitation data from the Rankin Station (orange). The figure also includes the precipitation inputs and the modelled hydrological inflow to the lake.

The primary difference between the simulation results using the Camp Station precipitation inputs and the Rankin Station precipitation input occurs in October 2024 where the precipitation recorded at the Camp Station is substantially higher than that recorded at the Rankin Station. This results in significantly more inflow to the lake and correspondingly higher lake levels during that period. It should be noted that there are also notable differences in measured precipitation at the Camp and Rankin stations during the period from January to May 2025, but this precipitation was all accumulated as snow so there was not corresponding inflow or lake level response to these events. In both precipitation scenarios, the model over-estimates the lake level during the period from October 2024 to January 2025 but, aside from the period in October when the lake level is exceeded, the slope of the receding limb of the lake water level curve is closely matched by both model scenarios.

Overall, the model successfully reproduces the seasonal lake-level pattern, capturing two major peaks—in October 2024 and June 2025—and a smaller peak in August 2025. The October 2024 peak was driven by rainfall events, whereas the June 2025 peak was driven primarily by snowmelt.

In September 2024, at the beginning of the calibration period, the modelled lake level increases sooner than the measured lake level because the model is unable to reproduce the sudden drops in the lake level during periods where there is no precipitation. While simulated inflows to the lake exhibit similar fluctuations during this period (due to the absence of rainfall), the discrepancy between the modelled and measured lake level is likely due to underestimated outlet discharge rates. Higher discharge rates would lower the simulated lake levels more rapidly and better match the observed pattern.

Between January and May 2024, the modelled lake level declines more rapidly than the measured lake level. By late May, the simulated lake level is approximately 0.1 m lower than the measured level. Since the inflow to the lake is at or near zero during this period, the lake-level changes are controlled solely by outflows at the two outlets plus the mine withdrawal. This suggests that the rating curves derived from open-water-season measurements do not adequately represent winter conditions which are likely influenced by the impact of ice cover on the water level, and the impact of ice cover on the outflow at the outlets. Furthermore, while the model does account for snow accumulation and melting, it does not account for the transformation of the lake water to ice cover and the associated 'storage' of lake water in the ice cover. Thus, the lower modelled lake level during the winter months is attributed to ice cover effects which are not accounted for in the outflow rating curves (i.e. the model is over-estimating the outflow from the lake during winter periods).

In June 2025, the modelled and measured lake level closely matches during the peak snowmelt period but the measured lake level plateaus at a level of 51.78 m for approximately two weeks and then abruptly jumps to a peak water level of 51.82 m in late June, while the modelled water level continuously rises to peak water level of 51.81 m without plateauing. Neither the rainfall data nor the temperature data suggest any explanation for the plateauing or the sudden increase at the end of June. However, with such a large basin and so many tributaries, this type of response may suggest that inflow from a large tributary subbasin may have been temporarily obstructed in early June and then released later in the month—processes not represented in the hydrologic model.

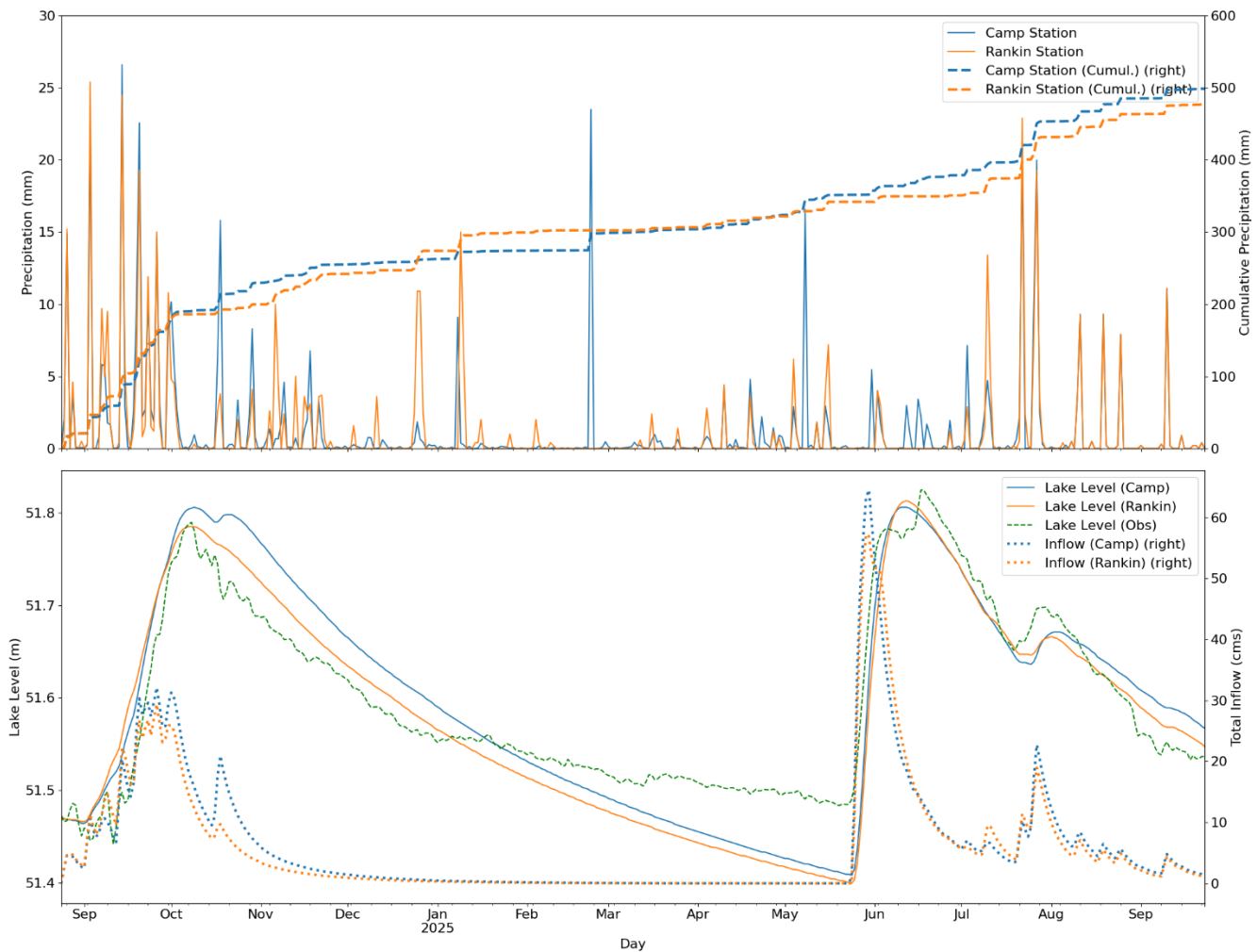


Figure 5-1 Modeled and Measured Lake Level (Aug 25, 2024 to Sep 24, 2025)

5.4 Model Validation Result

The modelled and measured lake levels for the validation period are shown in Figure 5-2. As the precipitation data at Camp Station is only available for short period of time in 2000, the model simulation used the precipitation and temperature data from the Rankin Station. The freshwater withdraw and effluent discharge were removed from the model as it is unknown whether they were operated during the validation period.

The modelled lake level shows a similar pattern and timing as the measured lake level during the validation period, but the modelled peak lake level during the initial snow melt period is significantly lower than the measured peak lake level in 1997, 1999, and 2000. The large difference in peak lake water level can be attributed to one or all of the following:

- a) The elevation datum for the lake levels during this period was assumed (see Section 2.3), so the difference in measured vs. modelled peak lake levels may be an indication that the assumed datum was too low.
- b) The model does not account for lake water that is transformed to ice and stored in the thick ice cover. A rapid melt of the ice cover would provide a sudden rise in the lake level that is not accounted for by snow melt contributions from the subbasins.

- c) The data is more than 20 years old and the rating curves for the outlets may have been different at that time

It is also interesting to note that the modelled vs. measured lake level during the period of January to May 2000 behaves similar to the period of January to May 2025, whereby the modelled lake level drops continuously as governed by the rating curves for the outlets, while the measured lake level drops at a much slower rate and even plateaus during some periods. This difference supports the above assertion that the current rating curve is either incorrect at low lake levels, and/or that lake ice cover and melting influence the outflow from the lake.

While the model validation is under-estimating the peak lake water level during the spring snowmelt, the potential root causes of the error in the model (i.e. lake elevation datum, lake ice cover dynamics, and/or old data and rating curves differences) cannot be addressed within the scope of this study. Furthermore, any adjustments to the model to increase the lake level during peak snow melt period for the model validation will further compromise the over-estimation of the measured lake level during the peak snow melt period for the model calibration.

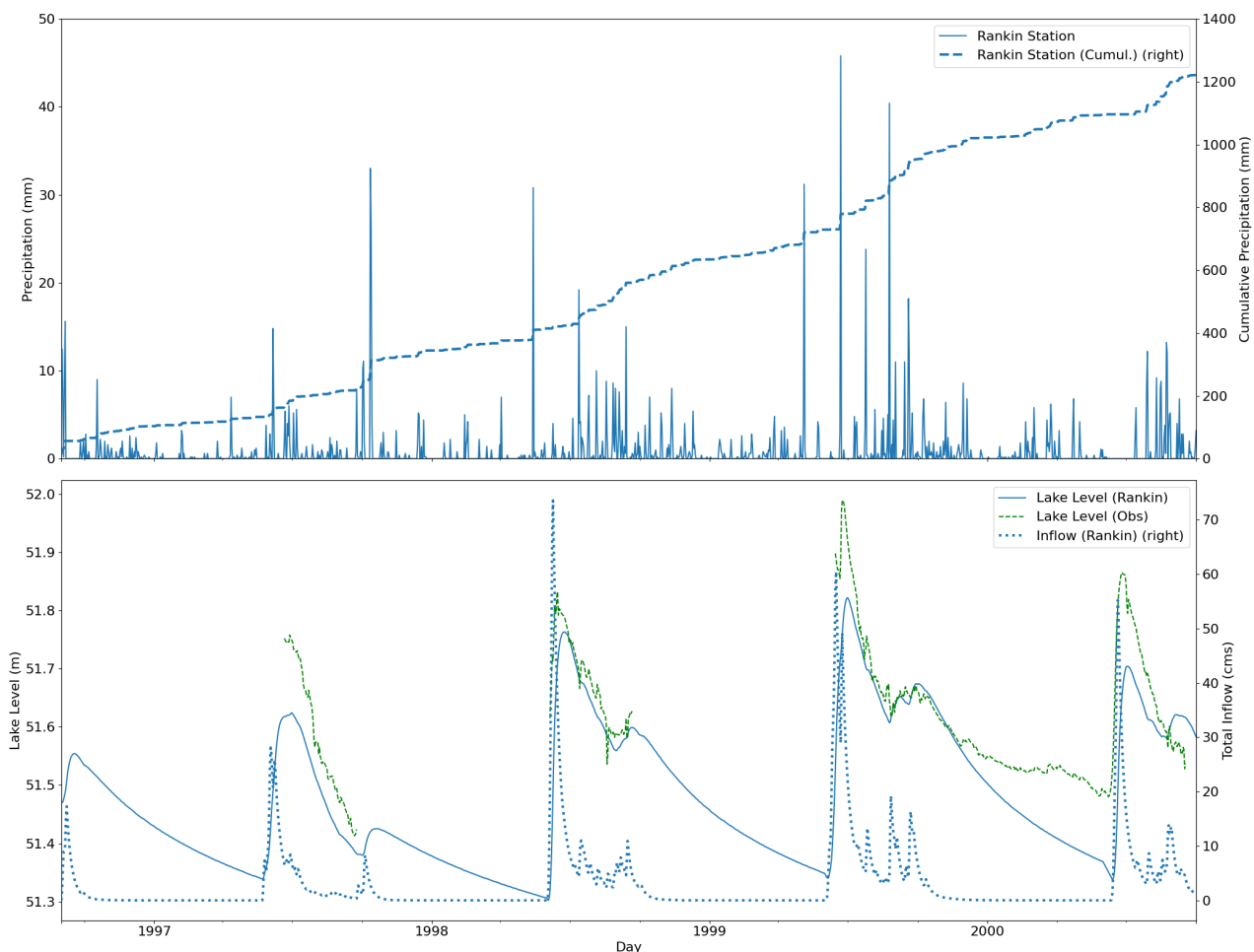


Figure 5-2 Modeled and Measured Lake Level (Sep 1, 1996 to Oct 1, 2000)

6 Projected Inflow and Lake Levels for the Future Mine Operations Period (2026-2036)

The calibrated and validated model was used to estimate lake inflows for the period from 2026-2036 using daily climate projections provided by Agnico Eagle (948-021-Meliadine-Climate-Change-Database.xlsx). The climate data contains daily climate data for the period from 2020 – 2120 for 3 potential climate change scenarios:

1. RCP 4.5: Assumes GHG concentrations in the atmosphere peak in 2040 and then begin to decline.
2. RCP 6.0: Assumes GHG concentrations in the atmosphere peak in 2080 and then begin to decline.
3. RCP 8.5: Assumes GHG concentrations in the atmosphere continue to rise through the 21st century.

The climate data includes:

- Total Precipitation
- Minimum Air Temperature
- Maximum Air Temperature
- Minimum Relative Humidity
- Maximum Relative Humidity
- Net Radiation Flux
- Wind Speed

For the hydrological model input, the Total Precipitation values were used directly in the model, and the Minimum Air Temperature and Maximum Air Temperature values were used to calculate an average daily Air Temperature.

Figure 6-1 below shows the precipitation for the period of 2026-2050. The daily precipitation and accumulative precipitation are also included in the figure. The precipitation of RCP 4.5 and RCP 6.0 have similar pattern and accumulative values for the period of interest in this study. Beginning in 2031, RCP 8.5 has consistently less precipitation than RCP 4.5 and RCP 6.0. An anomalously large precipitation event stands out on July 16, 2039 with 86 mm for RCP 4.5 and 57 mm for RCP 6.0 (this event was not present in the RCP 8.5 data set). In 2042, the RCP 4.5 and RCP 6.0 precipitation is significantly higher than in most years, while the precipitation for RCP 8.5 is significantly lower than in most years. Finally, in 2043, there is an anomalously large rainfall event late in the year.

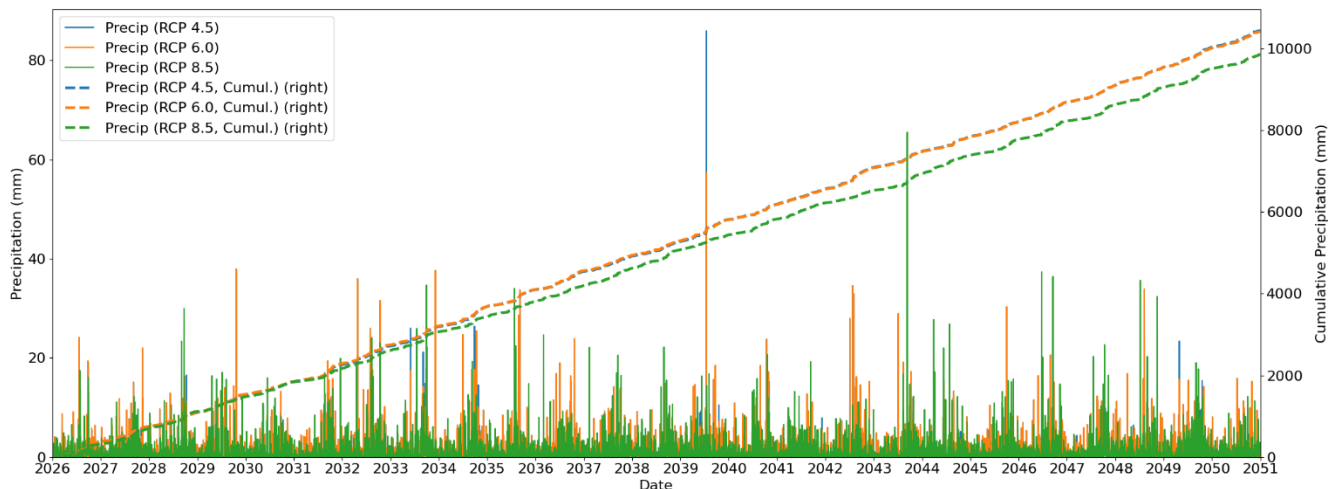


Figure 6-1 Precipitation from 2026 to 2050

For the historical period of 2020 to 2025, the cumulative precipitation from the future climate change data set was compared to the record at the Rankin Station as shown in Figure 6-1. It shows that all three climate change scenarios have more precipitation than what was observed at the Rankin Station, so these future climate scenarios may be biased towards more precipitation. However, this observation is inconclusive due to the relatively short period of comparison.

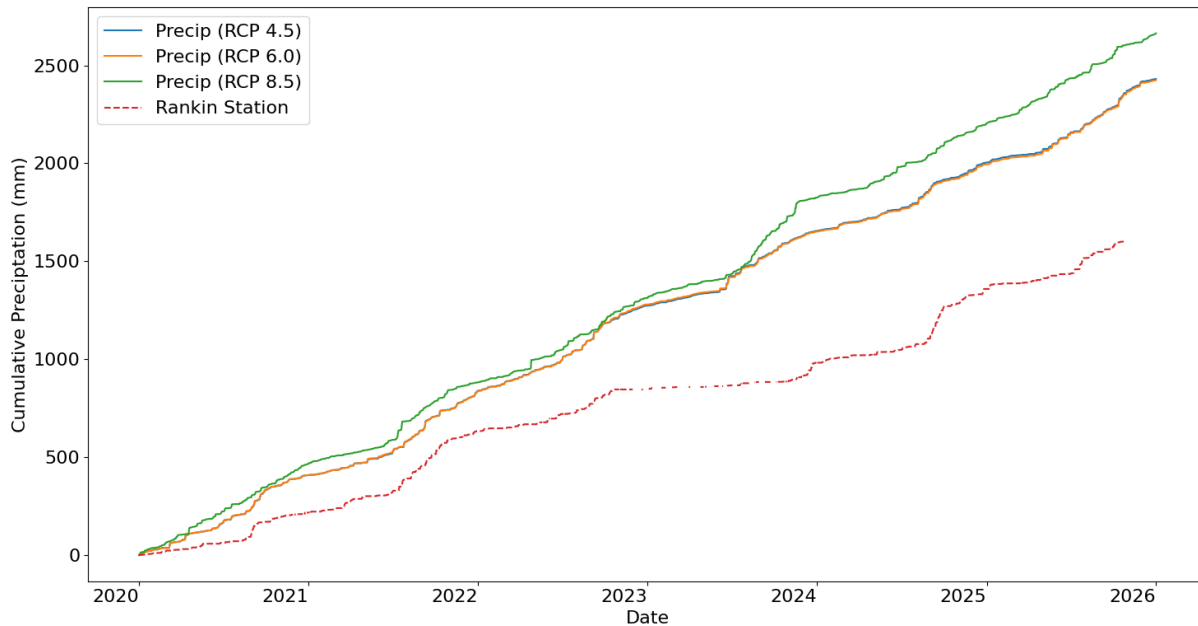


Figure 6-2 Accumulative Precipitation from 2020 to 2025 for Climate Change Scenarios and Rankin Station

The potential evapotranspiration (PET) was calculated using the Priestley-Taylor (PT) and Penman-Monteith (PM) method with input from the climate data. The Priestley-Taylor method used temperature and net radiation with a coefficient of 1.26, while the Penman-Monteith method used temperature, relative humidity, net radiation and wind speed. The calculated values were summarized as average monthly values and compared in Figure 6-2. For comparison, the monthly evapotranspiration values listed in the Baseline Report (Golder Associates, 2012) were also included. Figure 6-3 compares the average annual PET values. This shows that Penman-Monteith method produces higher PET than Priestley-Taylor method for all three climate change scenarios. Sublimation was considered in Penman-Monteith method during winter when Priestley-Taylor PET are zeros. The monthly evaporation in the Baseline Report is higher in July, August and September is lower in June. The average annual PET plot shows the values from the Baseline Report are higher than the values calculated by Priestley-Taylor method and lower than the value from Penman-Monteith method. Since the Penman-Monteith method uses all of the climate data and accounts for ET throughout the year, it was used to run the future scenario simulations.

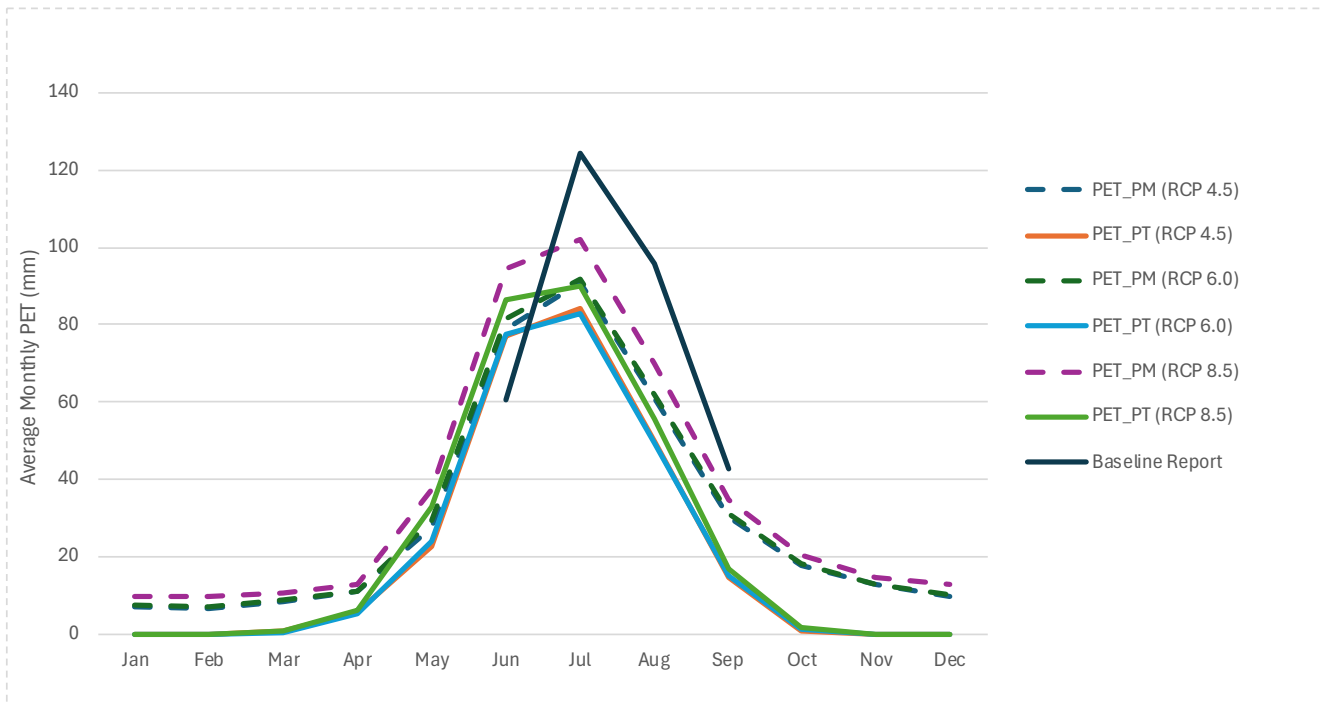


Figure 6-3 Average Monthly PET

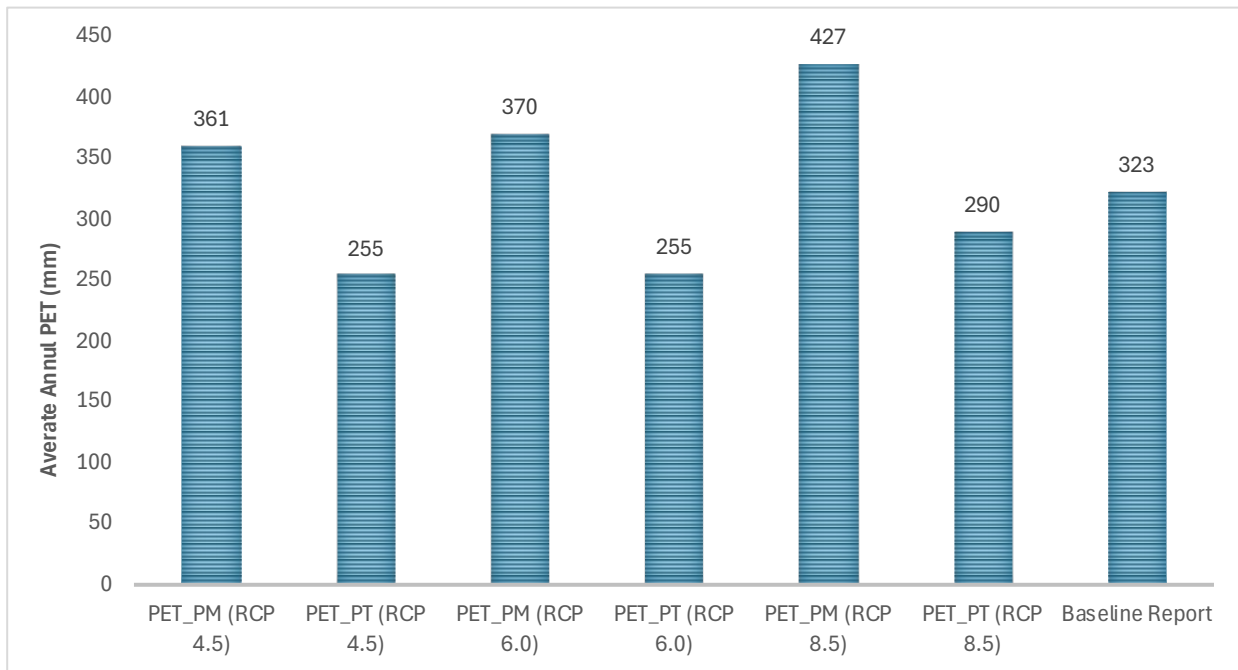


Figure 6-4 Average Annual PET

6.1 Future Model Scenarios

The Meliadine Lake hydrological model was run for the scenarios described in the following table:

Scenario ID	Climate Change Scenario	Annual Withdrawal (m ³)	Annual Effluent Discharge (m ³)
1_Ex_4.5	RCP 4.5	519,502	861,476
2_Ex_6.0	RCP 6.0	519,502	861,476
3_Ex_8.5	RCP 8.5	519,502	861,476
4_Max_4.5	RCP 4.5	1,110,296	861,476
5_Max_6.0	RCP 6.0	1,110,296	861,476
6_Max_8.5	RCP 8.5	1,110,296	861,476

The first three scenarios represent the existing freshwater withdrawal (519,502 m³/yr) and existing effluent discharge (816,476 m³) under potential future climate change conditions, while the last three scenarios represent the maximum freshwater withdrawal (1,110,296 m³) and existing effluent discharge under potential future climate change conditions. The existing annual freshwater withdrawal and effluent discharge were assumed to be the same as reported in the 2024 monthly water volume records (Angico Eagle, 2024). For the purposes of this project, the proposed maximum annual withdrawal of 1,110,296 m³ was distributed throughout the year using the same proportional distribution as the 2024 monthly extraction rates reported in the monthly water volume records (Angico Eagle, 2024).

For each scenario, the freshwater withdrawal and effluent discharge are applied for the period from 2026-2036 and then both withdrawal and discharge are set to zero for the post-closure period of 2037-2041.

6.2 Model Results

Figure 6-4 to Figure 6-6 presents a comparison of the lake inflow and water levels for the existing freshwater extraction vs. the proposed maximum freshwater extraction scenario for each climate change scenario, while Figure 6-7 presents a comparison of the lake inflow and lake water level for the maximum freshwater extraction scenario for each of the climate change scenarios. A summary of the results is presented in Table 6-1.

As seen in Figure 6-4 to Figure 6-6 and summarized in Table 6-1, there is no meaningful difference in the lake levels between the existing freshwater extraction conditions and the proposed maximum freshwater withdrawal conditions (representing a difference in annual freshwater withdrawal of 590,794 m³). This result is not surprising because the increase from existing annual freshwater withdrawal to the proposed maximum annual freshwater withdrawal is 590,794 m³, which represents less than 0.5% of the average annual inflow to the lake. Similarly, the proposed 10,000 m³ increase to the maximum annual freshwater withdrawal represents less than 0.01% of the average annual inflow to the lake, so the effect of this proposed increase to the maximum annual freshwater withdrawal is negligible.

In comparing the water levels for the maximum freshwater withdrawal conditions for each climate change scenario, Figure 6-7 shows that the lake water level from RCP 4.5 and RCP 6.0 are very similar throughout the future climate period, with higher lake water levels than RCP 8.5 during the snow melt period for the majority of the years, while RCP 8.5 produces higher lake water levels during summer/fall for many years. However, the overall impact of the climate change scenario on the average annual water level in the lake for the period of interest is also negligible (approximately 1 cm).

Table 6-1 Statistics of Lake Water Level and Outflow for the Period from 2026-2036

Scenario	Average Maximum Peak Water Level (Spring)	Average Maximum Peak Water Level (Fall)	Average Annual Water Level (masl)	Average Lake Inflow (m3)
1_ Ex_ 4.5	51.868	51.726	51.560	186M
2_ Ex_ 6.0	51.868	51.727	51.561	187M
3_ Ex_ 8.5	51.826	51.715	51.554	166M
4_ Max_ 4.5	51.868	51.726	51.560	186M
5_ Max_ 6.5	51.868	51.726	51.560	187M
6_ Max_ 8.5	51.825	51.714	51.553	166M

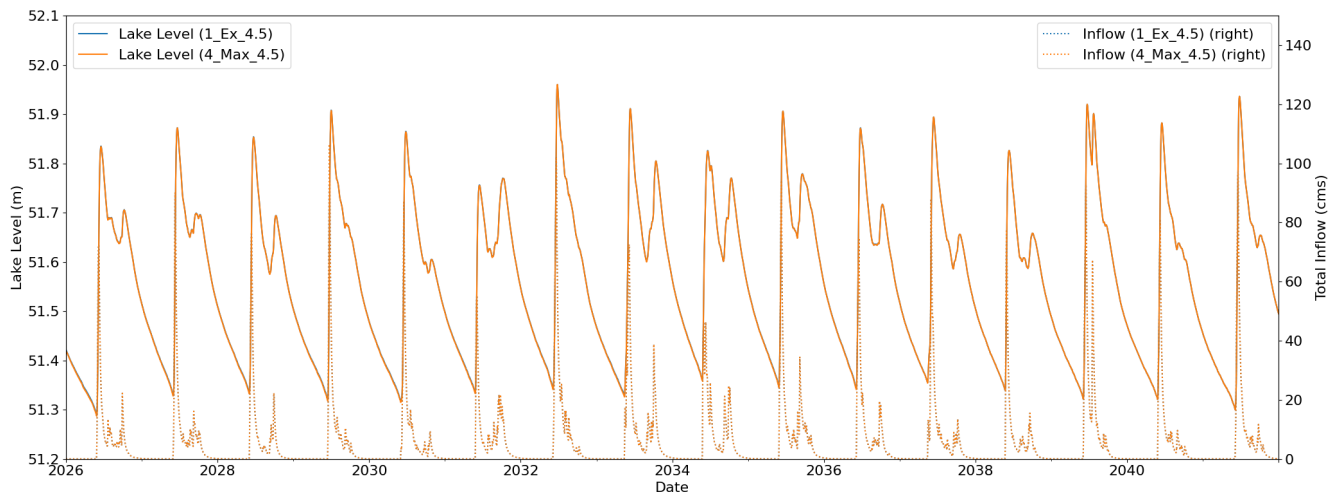


Figure 6-5 Meliadine Lake Level and Inflow for Existing and Maximum Withdrawal Scenarios (2026-2036, RCP 4.5)

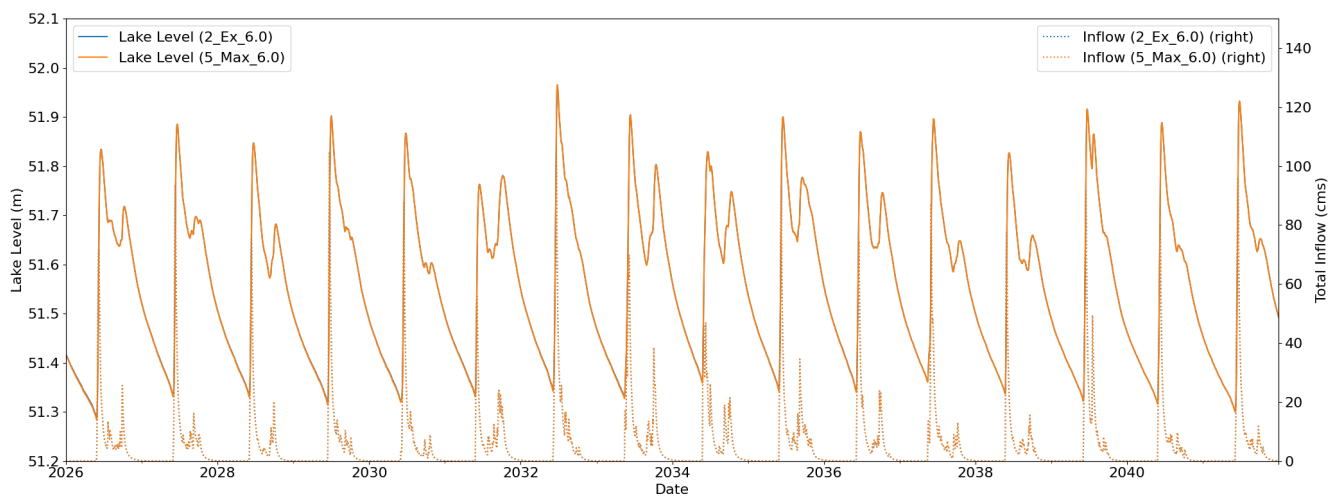


Figure 6-6 Meliadine Lake Level and Inflow for Existing and Maximum Withdrawal Scenarios (2026-2036, RCP 6.0)

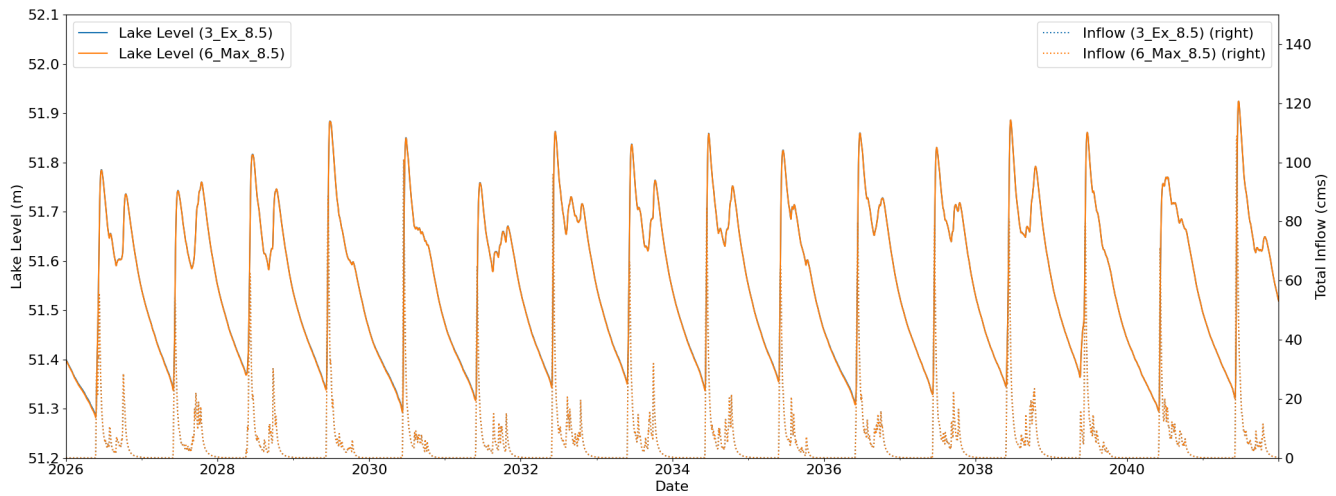


Figure 6-7 Meliadine Lake Level and Inflow for Existing and Maximum Withdrawal Scenarios (2026-2036, RCP 8.5)

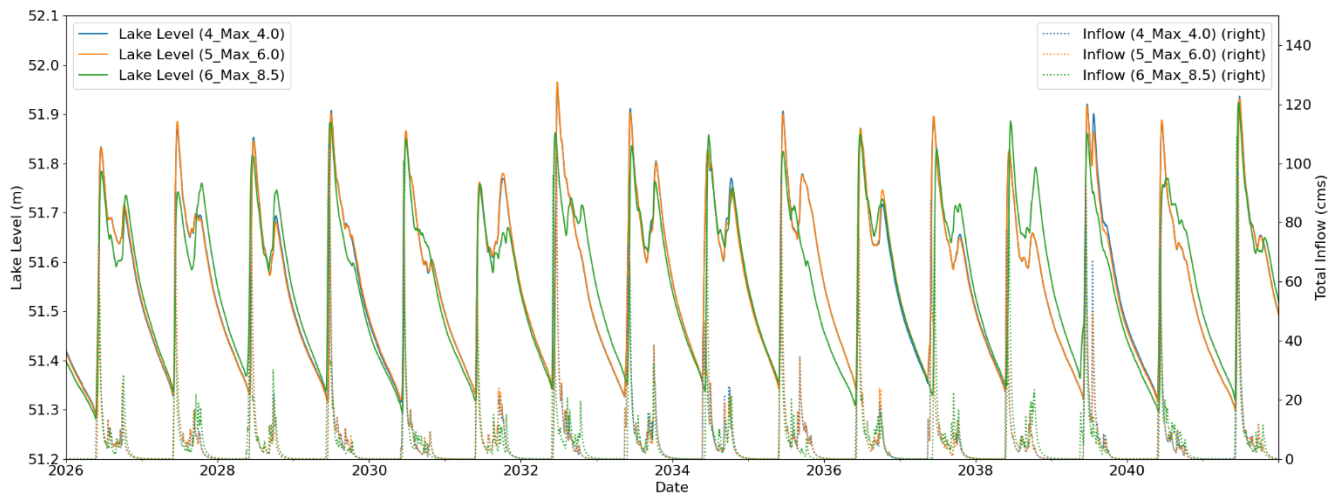


Figure 6-8 Meliadine Lake Level and Inflow for Maximum Withdrawal Scenario (2026-2036, RCP 4.5, RCP 6.0 and RCP 8.5)

7 Mine Closure 2037-2043

The calibrated and validated model was used to estimate lake inflows for the mine closure period from 2037-2043 using the same future climate data and data processing and preparation approach described in Section 6.

7.1 Model Scenarios

The Meliadine Lake hydrological model was run for the proposed mine closure scenario with freshwater withdrawal of 8,700,000 m³ per year during the period of June 15 to September 30 each year (80,556 m³/day). This scenario was evaluated for all three climate scenarios (RCP 4.5, RCP 6.0, and RCP 8.5).

7.2 Model Results

A summary of the results is presented in Table 7-1 while Figure 7-1 presents a comparison of the Meliadine Lake inflow and water level for the proposed mine closure scenario for each of the climate change scenarios. As shown, the overall differences between the different climate change scenarios is not very significant with the exception of the average annual inflow to the lake being considerably less for the RCP 8.5 scenario. This was to be expected given the declining trend in the cumulative precipitation shown in Figure 6-1. With respect to the differences between the 2026-2036 period and 2037-2043 period, the peak water levels are very similar but the average annual water level in the mine closure period drops by approximately 2 cm.

As shown in Figure 7-1, the influence of the climate change scenarios is more obvious within each year, but the time period of 7 years is too short to draw any strong conclusions about potential trends between the different climate scenarios. The last two years are particularly notable because the RCP 8.5 water level results are significantly different than the RCP 4.5 and RCP 6.0 results. However, it should be emphasized that this is not a prediction of what will actually happen in those specific years. It's merely a coincidence that the climate change data introduced some anomalous precipitation data in 2042 and 2043. Figure 6-1 shows that the long-term trend of cumulative precipitation beyond 2042 and 2043 is relatively stable but with some interannual differences from one year to the next.

Table 7-1 Statistics of Lake Water Level and Outflow for Mine Closure Analysis

Climate Scenario (ID)	Average Maximum Peak Water Level (Spring)	Average Maximum Peak Water Level (Fall)	Average Annual Water Level (masl)	Average Lake Inflow (m ³)
RCP 4.5 (4 JS 4.5)	51.875	51.665	51.542	187M
RCP 6.0 (5 JS 6.0)	51.875	51.660	51.540	184M
RCP 8.5 (6 JS 8.5)	51.814	51.669	51.533	166M

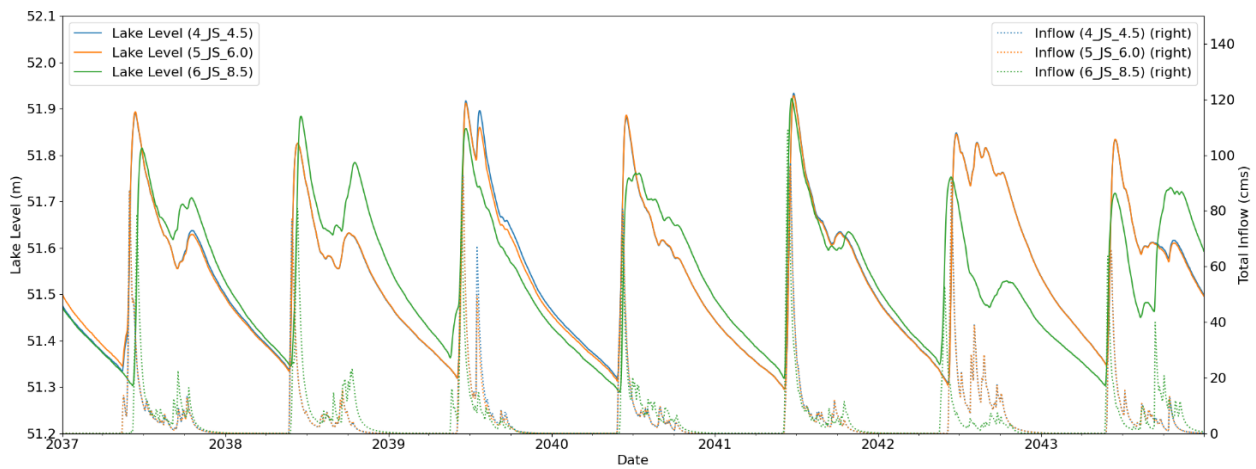


Figure 7-1 Meliadine Lake Level and Inflow for June-Sept Withdrawal Scenario (2037-2043, RCP 4.5, RCP 6.0 and RCP 8.5)

8 Conclusions

In this project, a HEC-HMS hydrology model was developed for the entire Meliadine Lake watershed using updated bathymetry, lake level and climate data. The modelled inflow to Meliadine Lake was calibrated using lake level data collected from 2024-2025 and was validated using historical data from 2014 FEIS. The model was then used to quantify the inflow to Meliadine Lake over duration of the Project between 2026-2041 while considering three climate change scenarios.

The modelled lake levels showed a very good match to the measured peak lake levels for the calibration period with some divergence during the winter period that is likely caused by ice cover influences on the outflow from the lake. The model performed similarly for the validation period, where it demonstrated a similar pattern as the measured lake level but it under-estimated the peak lake water level during a short duration at the beginning of the snow melt period for three of the four years. The difference in peak lake water level can be attributed to deficiencies identified with the historical data collected during the baseline studies (predominantly the lack of a reliable elevation datum, and lack of a rating curve for ice cover conditions). The data gaps are anticipated to improve over time as more hydrology data is collected and incorporated into the model.

Overall, the model has shown that it can reliably predict seasonal changes in the inflow to Meliadine Lake and the associated changes in lake water levels in a manner that is suitably reliable for estimating the relative impact of increasing the maximum annual freshwater withdrawal from the lake by 10,000 m³.

The impact of the proposed maximum annual freshwater withdrawal was evaluated using the calibrated hydrological model to predict Meliadine Lake water levels during the mine operating period of 2026 to 2036 using two different mine closure scenarios; (1) using the existing annual freshwater withdrawal of 519,502 m³; and (2) using the proposed maximum annual freshwater withdrawal of 1,110,296 m³. Both of these withdrawal scenarios were run for three different potential future climate change scenarios (RCP 4.5, RCP 6.0 and RCP 8.5). The results of these scenarios show that the proposed maximum annual freshwater withdrawal will produce no meaningful difference in the lake levels compared to existing conditions. Similarly, increasing the annual freshwater withdrawal by 10,000 m³ will have no measurable effect on the lake water levels.

The impact of the proposed annual freshwater withdrawal of 8.7M m³ during the mine closure period of 2037-2043 was also evaluated using the hydrological model to estimate the lake level drawdown caused by the withdrawal. The model was run for three potential future climate change scenarios (RCP 4.5, RCP 6.0 and RCP 8.5). The modelling results demonstrated that the impact on the peak water levels was generally less than 1 cm while the impact on the average annual lake level was less than 2 cm.

The modelled inflows to Meliadine Lake for all scenarios were provided for use in the lake hydrodynamics and water quality modelling study.

9 References

Agnico Eagle. (2024). *Meliadine Gold Mine 2024 Annual Report*. Nunavut: Agnico Eagle.

Golder Associates. (2012). *SD 7-1 Auqatics Baseline Synthesis Report, 1994 to 2009 - Meliadine Gold Project, Nunavut*.

HEC-HMS Team. (2025, Jan 29). *HEC-HMS Tutorials and Guides*. Retrieved from Hydrologic Engineering Center: <https://www.hec.usace.army.mil/confluence/hmsdocs/hmsguides/applying-transform-methods-in-hec-hms/estimating-clark-unit-hydrograph-parameters/estimating-time-of-concentration-storage-coefficient>